

BAP v2: An Enhanced Task Framework for Instruction Following in Minecraft Dialogues

Prashant Jayannavar*
University of Illinois
Urbana-Champaign

Liliang Ren**
Microsoft

Marisa Hudspeth**
University of Massachusetts Amherst

Charlotte Lambert†**
University of Illinois
Urbana-Champaign

Ariel Cordes†**

Elizabeth Kaplan†**
Amazon

Anjali Narayan-Chen†**
Amazon AGI

Julia Hockenmaier
University of Illinois
Urbana-Champaign

*Interactive agents capable of understanding and executing instructions in the physical world have long been a central goal in AI research. The **Minecraft Collaborative Building Task (MCBT)** provides one such setting to work towards this goal (Narayan-Chen, Jayannavar, and Hockenmaier 2019). It is a two-player game in which an Architect (A) instructs a Builder (B) to construct a target structure in a simulated Blocks World Environment. We focus on the challenging **Builder Action Prediction (BAP)** subtask of predicting correct action sequences in a given multimodal game context with limited training data (Jayannavar, Narayan-Chen, and Hockenmaier 2020). We take a closer look at evaluation and data for the BAP task, discovering key challenges and making significant improvements on both fronts to propose **BAP v2**, an upgraded version of the task. This will allow future work to make more efficient and meaningful progress on it. It comprises of: (1) an **enhanced evaluation benchmark** that includes a cleaner test set and fairer, more insightful metrics, and (2) additional **synthetic training data** generated from **novel Minecraft dialogue and target structure simulators** emulating the MCBT. We show that the synthetic data can be used to train more performant and robust neural models even with relatively simple training methods. Looking ahead, such data could also be crucial for training more sophisticated, data-hungry deep transformer models and training/fine-tuning increasingly large LLMs. Although modeling is not the primary focus of this work, we also illustrate the impact of our data and training methodologies on a simple LLM- and transformer-based model, thus validating the robustness of our approach, and setting the stage for more advanced architectures and LLMs going forward.*

* Corresponding author; E-mail: paj3@illinois.edu

** Work done while author was a graduate student or undergraduate intern at UIUC

† Equal contribution

1. Introduction

There has long been interest in developing interactive agents that can communicate with humans about and operate within the physical world (e.g., Winograd (1971)). The goal for these agents is not only to engage in rich natural language dialogue, but also to ground it to physical objects, and execute instructions in the real world. We work toward this goal using **Minecraft** (<https://minecraft.net/>), a popular multiplayer game where players control avatars to navigate a 3D world and build structures from block-like materials. Minecraft, in recent years, has garnered a lot of interest as an AI experimentation platform. Our previous work—the **Minecraft Collaborative Building Task (MCBT)** and the corresponding **Minecraft Dialogue Corpus (MDC)** (Narayan-Chen, Jayannavar, and Hockenmaier 2019)—was among the first to use it to study grounded task-oriented dialogue. Jernite et al. (2019) is another such example. More recent works, such as Mohanty et al. (2024), have been directly inspired by the MCBT. Additionally, there now exists a well-developed set of platform and tools that support AI experimentation within Minecraft, including Malmo (Johnson et al. 2016), Craftassist (Gray et al. 2019), TaskWorldMod (Ogawa et al. 2020), MC-Saar-Instruct (Köhn et al. 2020), IGLU GridWorld (Zholus et al. 2022), and Narayan-Chen, Jayannavar, and Hockenmaier (2019). The latter builds on the Malmo platform.

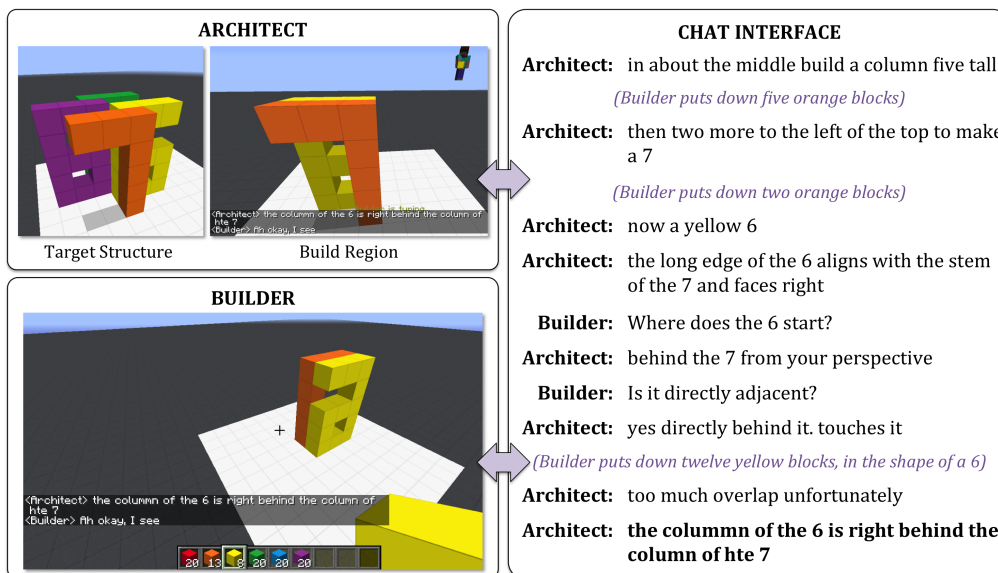


Figure 1: In the Minecraft Collaborative Building Task, the Architect (A) has to instruct a Builder (B) to build a target structure. A can observe B, but remains invisible to B. Both players communicate via a chat interface. (NB: We show B’s actions in the dialogue as a visual aid to the reader.)

The MCBT situates a dialogue task—designed to be asynchronous, asymmetric, and with minimal language constraints—in a simulated 3D Minecraft environment where participants, with constantly shifting perspectives, must refer to and modify a dynamic world. In this task, two players collaborate: an Architect (A) instructs a Builder (B) to construct a target structure using multi-colored blocks (Figure 1). The MDC comprises 509 human-human game logs for this task. Narayan-Chen, Jayannavar, and Hocken-

maier (2019) focus on generating Architect utterances, and Jayannavar, Narayan-Chen, and Hockenmaier (2020) focus on end-to-end neural models for building an automated Builder agent. The latter defined the challenging **Builder Action Prediction (BAP)** task, aimed at predicting the sequence of actions (block placements and/or removals) a human Builder performed at a specific point in a human-human game. Despite the task’s inherent challenges and limited training data, we demonstrate that models trained with a suitable amount of game history, enriched world representations, and a sufficient amount of synthetic, diversified data (via simple data augmentation techniques) yield promising initial results. We recap relevant prior work on the Minecraft Builder in Section 2. Building on this foundation, we next take a closer look at evaluation and training data for the BAP task, uncovering key challenges and making significant improvements on both fronts to propose **BAP v2**, an upgraded version of the task. This will allow future work to make more efficient and meaningful progress on it.

Given the inherent complexity of the task, we find that evaluation is nuanced and requires closer examination. We identify key challenges that hinder fair and insightful evaluation, then systematically address them. To this end, we introduce a new, cleaner v2 test set to replace the original legacy test set for evaluating BAP models (Section 3). We also refine the F1 metric, proposing a fairer variant that accounts for nuances in the data. The current evaluation, which relies solely on an aggregated and opaque F1 metric, lacks detailed insights into model behavior. To enhance insightfulness, we introduce additional metrics that measure specific model capabilities. Together, these contributions form the updated **BAP v2 evaluation benchmark** (Section 4).

Our work on evaluation highlights spatial reasoning as a key bottleneck in model performance, alongside the challenge of limited training data (even with the aforementioned data augmentation). Instead of merely collecting more data (which can be impractical/expensive in realistic scenarios for such complex situated dialogue tasks), we create additional diverse **synthetic training data** generated from **novel Minecraft dialogue and target structure simulators** that emulate the MCBT (Section 5). This data, though naturally simpler than it, is rich in spatial relations and referential expressions and we show that it can be successfully used to train better models, even with simple training methods (Section 6). We demonstrate that jointly training on combined synthetic and original BAP (augmented) data already improves performance. Further, a straightforward **Curriculum Learning** method provides an additional boost. Together, the synthetic and augmented BAP data form the **BAP v2 training set**. Looking ahead, such data could also be crucial for training more sophisticated, data-hungry deep transformer models and training/fine-tuning increasingly large LLMs. We provide a detailed analysis of model performance of our best performing model relative to the baseline in Section 7.

Although modeling is not the primary focus of this work, solely to test the robustness of our synthetic data and training methodologies and show their applicability to relatively contemporary model architectures, we experiment with very simple LLM (BERT)- and transformer-based variants of our neural models. The simplicity also allows us to assess whether/to what extent simpler LLMs like BERT and vanilla Transformers alone can already effectively handle the BAP task. Our results show that the synthetic data and training methodologies improve these models as well, validating the robustness of our approach (Section 6.3). Future work can build on these insights to explore more sophisticated LLMs and architectures while leveraging the BAP v2 framework.

Section 8 provides a detailed discussion on four topics – **an additional key challenge in BAP evaluation, the importance of evaluation on the synthetic data, relevant**

concurrent work, and broader implications of our work that go beyond BAP. The latter further highlights the potential impact of our work and directions for future research. Related work is covered in Section 9. We conclude and discuss future work in Section 10.

2. Prior Work on the Minecraft Builder

This section provides a high-level overview of the dataset, task, and baseline model, summarizing our prior work (Narayan-Chen, Jayannavar, and Hockenmaier 2019; Jayannavar, Narayan-Chen, and Hockenmaier 2020). We also introduce some necessary formalisms and figures for better exposition.

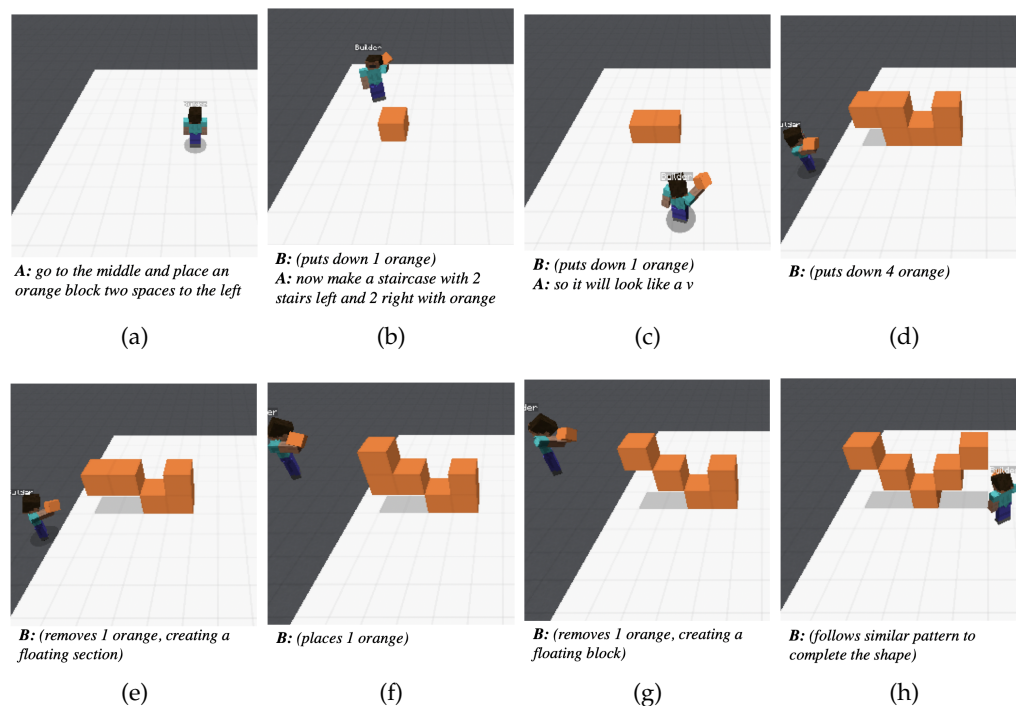


Figure 2: A sample sequence of human-human game states. The game starts with an empty board and an initial **A** instruction (a), which **B** executes in the first action sequence (b) by placing a single block. In (c), **B** begins to execute the next **A** instruction given in (b). However, **A** interrupts **B** in (c), leading to two distinct **B** action sequences: (b)–(c) (single block placement), and (c)–(h) (multiple placements and removals).

2.1 The Minecraft Collaborative Building Task and Dialogue Corpus

The **Minecraft Collaborative Building Task (MCBT)** is a two-player game in which player **A** (the *Architect*) has to instruct player **B** (the *Builder*) to create a copy of a *Target* structure that is only shown to **A**. **B** controls a Minecraft agent that is given a fixed inventory of blocks. **A** has access to two Minecraft windows, one which contains the *Target*, and one in which it can observe **B**'s actions. **A** remains invisible to **B** and cannot place blocks itself. **A** and **B** can only communicate via a text-based chat interface that

both can use freely throughout the game. The **Minecraft Dialogue Corpus (MDC)** consists of 509 human-human dialogues and game logs for this task, collected via a modification of the Malmo Minecraft client (Johnson et al. 2016). In the MCBT, each block **b** has one of six colors (red, orange, yellow, green, blue, purple), and **B** starts with an inventory of 120 blocks (twenty of each color) that it can place into or remove from a predefined BUILDREGION. Like in standard Minecraft, a discrete grid that is superimposed on the environment defines where blocks can be placed. In the Minecraft API, grid cells are indexed by integer-valued coordinates $c = \langle x, y, z \rangle$, where y indicates vertical height, but these coordinates are not exposed in the graphical interface, and players are unable to use them to identify specific cells in their conversations. Blocks can only be placed in empty grid cells that are either on the ground ($y = 1$) or adjacent to an existing block. If the Builder picks up (removes) a block, its grid cell becomes empty again, and the block returns to the inventory.

The games in the MDC consist mainly of **A** providing instructions, often involving multiple actions to be taken, and grounded in the Builder’s perspective, while **B** executes those instructions and resolves any confusion through clarification questions and further dialogue. They are based on 150 distinct target structures, split into disjoint test, training, and development sets such that training targets do not appear during test or development. Figure 1 (left) shows the perspectives seen by each player and a snippet of their conversation (right) taken from this corpus. The environment in which **B** operates contains the predefined BUILDREGION (shown as the white square on the ground). The task is complete when the *Built* structure inside the Build Region matches the *Target*, allowing for translations and rotations in the horizontal plane.

2.1.1 Features and Challenges. Since target structures can be fairly complex, Architects typically give step-by-step instructions (“*now a yellow 6*”) for different parts of the target. Builders should execute these instructions, but may also ask questions (“*Where does the 6 start*”) which the Architects has to answer (“*behind the 7 from your perspective*”). Architects may also need to identify and correct mistakes the Builder may have made (“*too much overlap unfortunately*”). **A** can move around freely, but remains invisible to **B** and views the structure from behind **B** when giving instructions. As a result, **A** instructions frequently include spatial relations, both between pairs of blocks or substructures (“*put ... on top of...*”), and relative to **B**’s current position and perspective (“*left*”, “*right*”). Humans also often use higher-level descriptions to refer to complex (sub)shapes (e.g. “*staircase*”, “*v*”). Due to the asynchronous nature of the dialogue, the Architect often talks while the Builder is placing blocks (“*so it will look like a v*”), leading to an apparent interruption of the Builder’s action sequences. Figure 2 shows an example from the MDC that highlights some of these challenges.

Floating blocks. Blocks do not need to be placed on the ground if their cell is adjacent to a supporting block. If that supporting block is later removed, the remaining block (and any structure supported by it) will “float” in place. Thus, placing floating blocks needs the placement and subsequent removal of such placeholder supporting blocks. Instructions for floating structures vary greatly, ranging from step-by-step instructions involving temporary supporting blocks to single-shot descriptions such as, simply, “*place a floating yellow block*”.

2.1.2 MCBT subtasks: Architect Utterance Generation and Builder Action Prediction. We define the **Architect Utterance Generation (AUG) Task** as the task of generating a suitable Architect utterance at any point in a human-human game at which the human

Architect produced an utterance (Narayan-Chen, Jayannavar, and Hockenmaier 2019), and the **Builder Action Prediction (BAP) Task** as the corresponding task of generating a suitable Builder action sequence (consisting of block placements/removals) at any point in a human-human game at which the human Builder placed or removed blocks (Jayannavar, Narayan-Chen, and Hockenmaier 2020). Although both of these tasks consider only a single turn, and assume the context of a game and dialogue between two human players, they are important first steps towards the creation of agents that can complete an entire game in the MCBT with a human counterpart.

2.2 The Builder Action Prediction (BAP) Task

The Builder Action Prediction (BAP) task is defined as the task of predicting the actions (block placements and/or removals) that a human Builder performed at a particular point in a human-human game. Games start with an empty board, and consist of an alternating sequence of dialogues D^t (which may each consist of a single utterance, or a back-and-forth exchange between the two players) and Builder actions A^t that result in an updated built structure S^t . Each action sequence A^t yields a **BAP item** $(\mathcal{H}^{t-1}, S^{t-1}, D^t, A^t, S^t)$ that consists of the **game history** \mathcal{H}^{t-1} that culminated in the **previous built structure** S^{t-1} , the **new dialogue** D^t , and the **new action sequence** A^t that resulted in the **new structure** S^t . Given \mathcal{H}^{t-1} , S^{t-1} , and D^t , BAP models M should predict an action sequence A_M^t that yields S^t .

Dataset statistics. The training, test and development splits of the MDC contain 3709, 1616, and 1331 items respectively, and the average sequence length of an action sequence (in the development set) is 4.3 (with a std. deviation of 4.5). Target structures in the test data do not appear in the training or development data.

Example. To illustrate this task, Figure 3 shows how the game snippet shown in Figure 2 corresponds to three different items for the BAP task. The leftmost columns in each figure display the (truncated) game history (S^{t-2} , D^{t-1} , S^{t-1} , and D^t), while the rightmost column shows the resulting built structure S^t . Columns are read top to bottom and left to right. Note that in this figure (and similar ones in this work), we use S_H instead of S for clarity (H indicates that the structure was built by a human, not a model). To highlight the effect of the final action sequence, previously placed blocks are shown in lighter colors, and each structure is rotated based on B’s gaze (only the yaw angle) at the end of the dialog snippet below it. B’s exact position and pitch angle are omitted for clarity. Any temporary supporting blocks are not shown as well. The game starts with an empty board S^0 , and an initial dialogue between the two players D^1 , and the first BAP item consists of predicting that first block placement A^1 (and consequent structure S^1) (Figure 3a). Then, another instruction follows, which the Builder executes by placing another block, resulting in the next structure to be predicted (Figure 3b), and the third instruction yields a complex action sequence that results in the desired v-shape structure (Figure 3c).

2.3 Formalizing the BAP task

The built structure. In Minecraft, blocks can be placed into the **cells** $\mathbf{c} = \langle x, y, z \rangle$ of a discrete 3D grid if \mathbf{c} is empty and either on the ground or adjacent to any cell \mathbf{c}' that contains a block. A cell $\mathbf{c} = \langle x, y, z \rangle$ is on the ground if its height $y = 1$, and

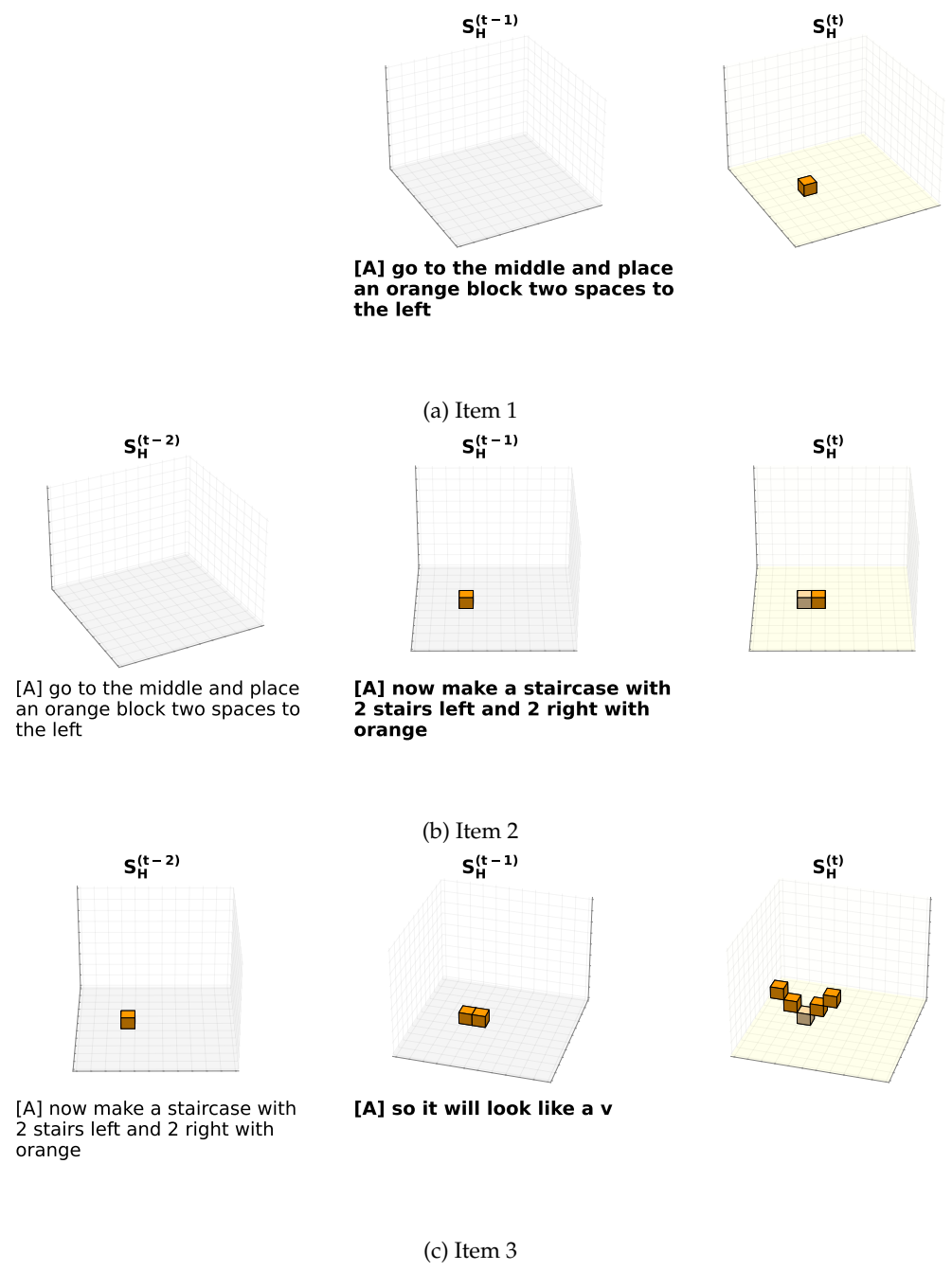


Figure 3: The snippet in Figure 2 corresponds to three BAP task items as shown.

is adjacent to any cell $\mathbf{c}' = \langle x', y', z' \rangle$ if they touch on one side.¹ In the MCBT, there

¹ Cells $\langle x, y, z \rangle$ and $\langle x', y', z' \rangle$ are adjacent if either $x = x' \pm 1, y = y',$ and $z = z',$ or $x = x', y = y' \pm 1,$ and $z = z',$ or $x = x', y = y',$ and $z = z' \pm 1$

are six different BLOCKCOLORS, and Builders place blocks inside a predefined **build region** BUILDREGION, an $11 \times 9 \times 11$ box that contains all grid cells $\mathbf{c} = \langle x, y, z \rangle$ from $\langle x_{\min}, y_{\min}, z_{\min} \rangle$ to $\langle x_{\max}, y_{\max}, z_{\max} \rangle$.² The current **Built structure** S can be represented as a list of blocks and their locations:

$$\begin{aligned} \text{BUILDREGION} &=_{\text{def}} \{ \mathbf{c} = \langle x, y, z \rangle \mid x_{\min} \leq x \leq x_{\max}, y_{\min} \leq y \leq y_{\max}, z_{\min} \leq z \leq z_{\max} \} \\ \text{BLOCKCOLORS} &=_{\text{def}} \{ \text{RED, ORANGE, YELLOW, GREEN, BLUE, PURPLE} \} \\ S &=_{\text{def}} \{ (\mathbf{c}, c) \mid \mathbf{c} \in \text{BUILDREGION}, c \in \text{BLOCKCOLORS} \} \end{aligned}$$

The Builder. The Builder can move freely around the environment. Since spatial relations in the instructions (“the block in front of you”, “to your left”) often depend on the Builder’s current location and viewpoint, we record the **position and pose/orientation of the Builder agent** $\text{POS}_{\mathbf{B}} = (\langle x_{\mathbf{B}}, y_{\mathbf{B}}, z_{\mathbf{B}} \rangle, \phi_{\mathbf{B}}, \gamma_{\mathbf{B}})$, where $\langle x_{\mathbf{B}}, y_{\mathbf{B}}, z_{\mathbf{B}} \rangle$ is a (real-valued) location (that may or may not be inside the build region), $\phi_{\mathbf{B}} \in [-90, \dots, +90]$ indicates a pitch (vertical rotation) and $\gamma_{\mathbf{B}} \in [-180, \dots, +180]$ a yaw (horizontal orientation). Note that $\text{POS}_{\mathbf{B}}$ is a critical component of game context as it dictates how spatial relations are interpreted.

The Builder’s actions. We specify Builder **actions** $a = (t, c, \mathbf{c})$ as triplets consisting of an action type $t \in \mathcal{T} = \{ \text{PLACE, REMOVE} \}$, a block color $c \in \text{BLOCKCOLORS}$, and a grid cell $\mathbf{c} = \langle x, y, z \rangle \in \text{BUILDREGION}$ whose state is changed by a .³ If a feasible action a is executed, it changes the built structure S to $S' \neq S$: $S \xrightarrow{a} S'$. A placement is feasible if \mathbf{c} is empty and either on the ground or adjacent to a non-empty cell, and results the addition of a c -colored block located in \mathbf{c} to S' . A removal action is feasible if S contains a block of color c in \mathbf{c} , and results the exclusion of that block from S' . When Builders follow an instruction, they execute an **action sequence** $A = \langle a^1, \dots, a^k \rangle$ for $k \geq 1$ and $a^1, \dots, a^k \in \text{ACTIONSPACE}$ that changes S to S' : $S \xrightarrow{A=\langle a^1, \dots, a^k \rangle} S'$. ACTIONSPACE is the set of all 7623 possible actions (7 actions available per cell in the $11 \times 9 \times 11$ build region—placing a block in one of 6 colors or removing a block).

2.4 Evaluating BAP models

To compare two action sequences, or to measure the change from S to S' , it is helpful to note that any action $a = (t, c, \mathbf{c})$ is undone by the **inverse action** $a^- = (t^-, c, \mathbf{c})$ where $t^- = \text{REMOVE}$ if $t = \text{PLACE}$, and $t^- = \text{PLACE}$ if $t = \text{REMOVE}$. Most commonly, this occurs when blocks are placed to serve as a necessary supporting block for a floating structure and removed in the same action sequence. These supporting blocks can be ignored since they do not occur in S' . Moreover, builders are free to use any color they wish, and can often choose among a variety of possible locations where to place these blocks. Human Builders are also prone to accidentally placing or removing blocks, but typically recognize and correct such mistakes immediately within the same action sequence. Finally, many structures do not require their blocks to be placed in a particular order. We can therefore transform any (feasible) action *sequence* A into a

² In the Minecraft Dialogue Corpus, the BUILDREGION’s horizontal coordinates x and z range from

$x_{\min} = z_{\min} = -5$ to $x_{\max} = z_{\max} = +5$ and vertical coordinates y range from $y_{\min} = 1$ to $y_{\max} = 9$.

³ Since the Malmo API can be used to move agents into positions in which a particular block is accessible to them, we ignore the Builder’s movement, and only consider its block placement and removal actions.

set of net actions A^{net} by first removing from A any actions a and their inverse a^- and turning the resulting (infeasible) sequence A' into a set A^{net} . The **distance** $\Delta(S, S')$ between two structures S and S' can then be defined as the number of net actions of any action sequence $A : S \xrightarrow{A} S'$ that changes S to S' : $\Delta(S, S') = |A^{\text{net}}|$, and any two action sequences A_1 and A_2 are **equivalent** ($A_1 \equiv A_2$), i.e. lead to the same subsequent structure, if they have the same set of net actions ($A_1^{\text{net}} = A_2^{\text{net}}$). We therefore evaluate BAP models against human Builders by comparing their respective net actions, A_M^{net} and A_H^{net} to compute a (strict) F1 score (we report a **micro-averaged** F1 score over all action sequences in the test/dev data):

Definition 1

Given a BAP item consisting of a (human) reference action sequence $A_H = \langle a_H^1, \dots, a_H^k \rangle$ that leads from S to S_H , corresponding to a reference net action set A_H^{net} , and a (model) predicted action sequence $A_M = \langle a_M^1, \dots, a_M^l \rangle$ that leads from S to S_M , corresponding to a predicted net action set A_M^{net} , **strict Precision, Recall and F1** scores assume that a Builder action $a_M^m = (t, c, \langle x, y, z \rangle) \in A_M^{\text{net}}$ is correct if and only if there is an equal reference action $a_H^h = (t, c, \langle x, y, z \rangle) \in A_H^{\text{net}}$:

$$\begin{aligned} \text{Strict Precision } P_{\text{strict}}(A_M^{\text{net}}, A_H^{\text{net}}) &= \frac{|(A_M^{\text{net}} \cap A_H^{\text{net}})|}{|A_M^{\text{net}}|} \\ \text{Strict Recall } R_{\text{strict}}(A_M^{\text{net}}, A_H^{\text{net}}) &= \frac{|(A_M^{\text{net}} \cap A_H^{\text{net}})|}{|A_H^{\text{net}}|} \\ \text{Strict F1 } F1_{\text{strict}}(A_M^{\text{net}}, A_H^{\text{net}}) &= \frac{2 \cdot P_{\text{strict}} \cdot R_{\text{strict}}}{P_{\text{strict}} + R_{\text{strict}}} \end{aligned}$$

2.5 Data Augmentation

Since the small size of the training set (3,709 examples) is a major limiting factor for training complex models, in Jayannavar, Narayan-Chen, and Hockenmaier (2020), we generated synthetic variants of the original game logs in the training data by combining three data augmentation techniques: **utterance paraphrasing** (synonym-based substitutions), **color substitution** (random color permutations across logs), and **spatial transformations** (rotating structures and Builder **B**) (details in appendix). Empirically, we found that increasing the training data to 14,836 (4x) items gave the best performance for our baseline model (Section 2.6). We will refer to this as the **original BAP (augmented) data**.

2.6 A CNN- and GRU-based baseline model

In Jayannavar, Narayan-Chen, and Hockenmaier (2020), we proposed a neural model for the BAP task. In this work, we build upon it and refer to it as **the baseline model**. The model (Figure 4) is based on a recurrent encoder-decoder architecture (Sutskever, Vinyals, and Le 2014; Cho et al. 2014) in which a GRU-based encoder (bottom left box) captures the game context (dialogue and action history) via GloVe embeddings (Pennington, Socher, and Manning 2014), and a CNN-based encoder (top left box) captures the world state at each time step. The world state encompasses the current built structure, action history and the Builder’s position and orientation. The decoder (right box) predicts one action per time step, based on the game history, the world state at that time, and the last action taken. It consists of another GRU backbone over action sequences (bottom right), and a multi-class classifier that reads in the output of the

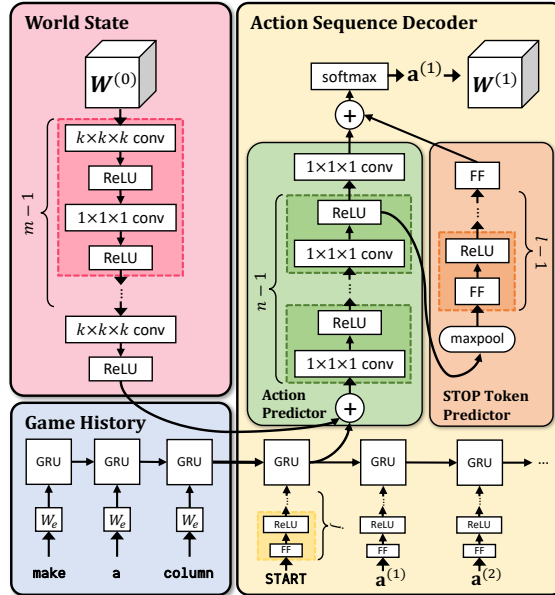


Figure 4: Baseline model in this work

GRU backbone as well as the world state encoding produced by the CNN to predict either the next action (block placement or removal) to be taken, or a special STOP token that terminates the action sequence. Actions are represented as feature vectors and embedded via feedforward layers before being fed to the decoder GRU. The world state representation gets updated and re-encoded after each predicted action. We train this model with teacher forcing and cross entropy loss on the original BAP (augmented) data, and use greedy decoding (max. sequence length of 10 actions) at test time. This yields an **F1 score of 21.2%** on the BAP test set. More details about the model are provided in the appendix.

3. Revisiting BAP Evaluation: A Cleaner Test Set

Since the MDC consists of real human-human game logs collected in a low-stakes, free-flowing setting with minimal constraints on the participants’ language and actions, rather than standalone instructions, this strategy does not always yield BAP items that are suitable for evaluation. First, Builders might move blocks even when no new instructions were given, or before it is completely clear what they should be building next (e.g. when the Architect only instructs the Builder to “*build a rectangle to the right of that*”, without specifying the size or color of the rectangle, let alone its orientation and distance to “*that*”). In such cases, the corresponding BAP items have an **unclear context**. Second, Builders occasionally make mistakes, and are frequently interrupted by the Architect, who may want to provide more information or simply affirm that the Builder’s actions are correct. In those cases, the BAP item’s action sequence may lead to an **incorrect structure**. Finally, when the board is empty, we observe that Architects do not always identify a specific location or orientation for the blocks to be placed, even when they clearly describe the structure to be built (e.g., the instruction “*place a red block on the ground*”). This likely occurs because there are no blocks on the board

or landmarks in the environment that could serve as spatial anchor to be mentioned, and because Architects are aware that the game only requires the Builder’s structure to match the Target as long as it appears anywhere inside the Build Region and in any orientation. In those situations, two different Builders might start the game by placing the same structure in two different locations and/or orientations and both might be correct, since the context provides **multiple (valid) interpretations**. This phenomenon arises almost exclusively with an **empty board**, since the blocks on a **non-empty board** and the current position of the Builder typically provide enough constraints for a clear instruction to only have a unique (valid interpretation) in that case. In this section, we perform an in-depth analysis of the items in the BAP test set that identifies these phenomena, and introduce a new, cleaner BAP test set that should be used to evaluate BAP models instead of the original, legacy test set. In the next section, we revisit the strict F1 metric, and define a fairer variant that accounts for the fact that some empty-board test items have multiple valid interpretations.

3.1 Annotating the test set

We manually annotate items in the test set so that we can identify cases that have to be distinguished for evaluation purposes. Annotators were asked to annotate all items in the same dialog in sequence. For each **non-empty board (NEB)** item, annotators were first asked whether the **context is clear and has a unique interpretation**, i.e. clearly specifies what structure to be built next, and there is only a single way of placing that structure on the board (as is typically the case when the board is not empty), or whether the **context is unclear**, i.e. it is unclear what the Builder should do next, either because more information is required, or no new instruction was given. For **empty board (EB)** items, annotators could also indicate that the **context is clear and has multiple interpretations**, i.e. it is clear what structure should be built, even though there are multiple possible placements or orientations within the build region, as is often the case when the board is empty. If the context is clear (with unique or multiple interpretations), a second question asked whether the built structure is **correct** or **incorrect**. Details about the annotation interface, the annotation workflow, the annotation tool, data collection setup, etc. are provided in the appendix. We now illustrate the resulting categories of BAP items with a few examples.

Clear context with unique interpretation and correct structure (Figure 5). It is clear what structure **B** should build next, only one such structure can be built, and the human Builder actually built that structure (Figure 5a). This can also arise when the board is empty (Figure 5b), since **B** is first made to stand at the bottom right corner of the board, and **A** clearly specifies the locations of the two blocks to be placed, given **B**’s new orientation.

Clear context with unique interpretation and incorrect structure (Figure 6). Here, it is clear what structure **B** should build next (and only one such structure can be built), but **B**’s actions did not result in that structure, perhaps because **B** got interrupted by **A**, or because **B** made a genuine mistake. In Figure 6a, **A** wants **B** to place two red blocks directly below the middle block of the top of the arch, but **B** only places one of those blocks. In Figure 6b, **A** wants **B** to place a red block diagonally above (“on top and in front of”) the topmost green block, but **B** places a red block in the wrong location. In the next BAP item from that dialog (Figure 6c), **A** tries to correct **B**’s mistake, but **B** now places two red blocks, only one of which should be there in the final structure.

Clear context with multiple interpretations and correct structure (Figure 7). When the board is empty, it is often clear what structure **B** should build next, but the placement and orientation of that structure may not have been uniquely specified. In this case, the context is clear, although it can be (correctly) interpreted in multiple ways.

Unclear context (Figure 8). Finally, some action sequences occur in contexts in which it is unclear what the Builder should do next. In Figure 8a, it is unclear what exact location **A** implies by “the side of the red”. In Figure 8b, **A** only signals they had made an error, but it is unclear what the error is or what its recency is and **A** does not provide any information that would allow **B** to correct the error.

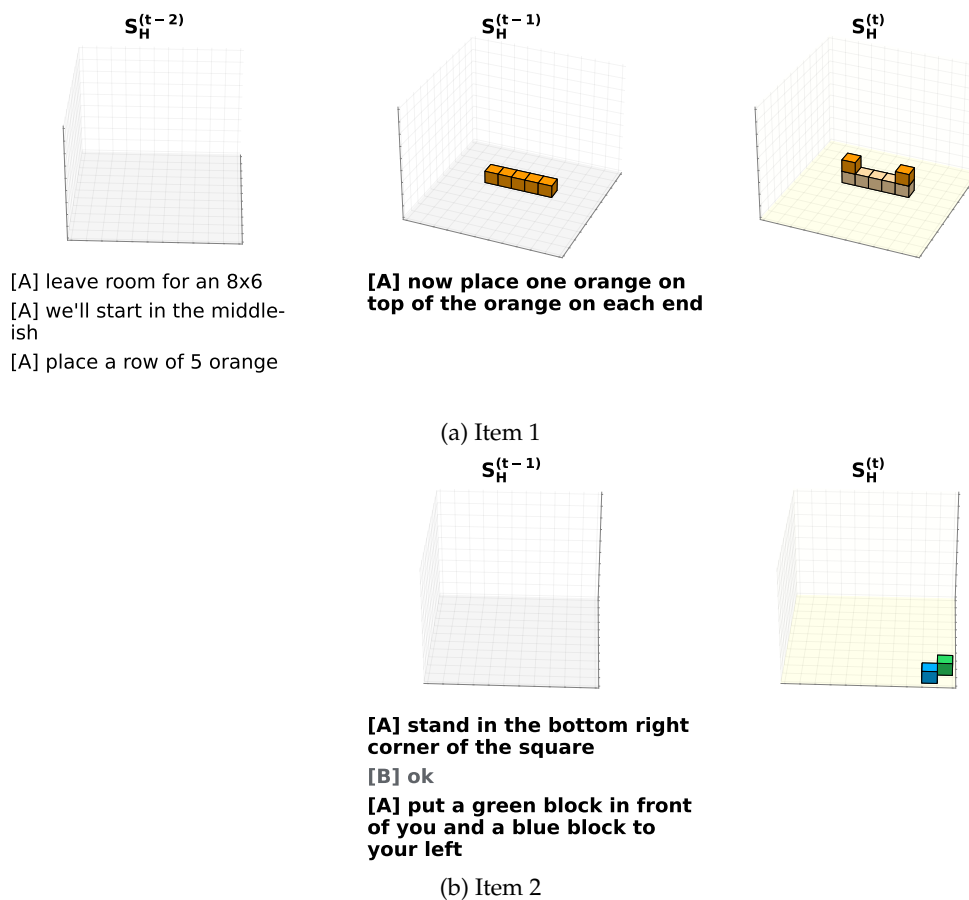


Figure 5: Clear context with unique interpretation and correct structure

3.2 Creating a clean test set

To obtain a clean BAP test set, we remove all items with unclear contexts, as the the correctness of the built structure cannot (and should not) be assessed for the BAP task. We also automatically fix/replace incorrect structures that can be fixed in such manner, and remove the items with structures that can't be fixed. This results in a new, **BAP**

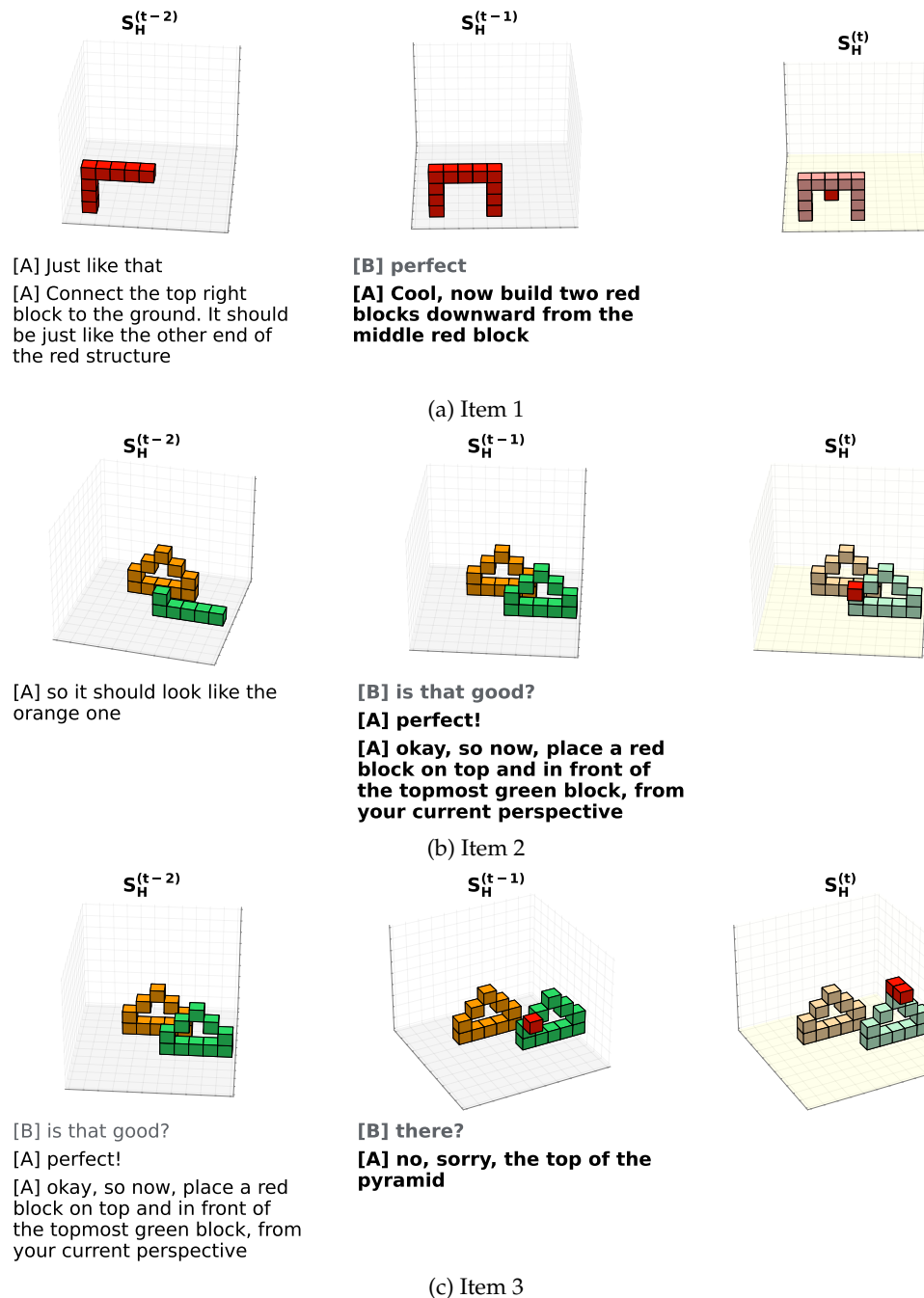
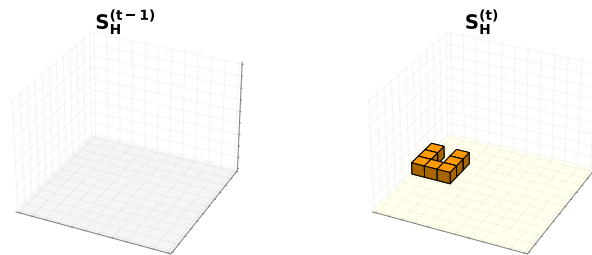


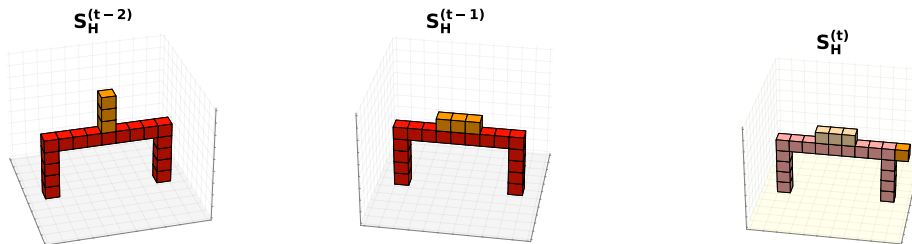
Figure 6: Clear context with unique interpretation and incorrect structure

v2 test set that contains only items with clear contexts and correct structures, and thus suitable for fairer BAP evaluation.



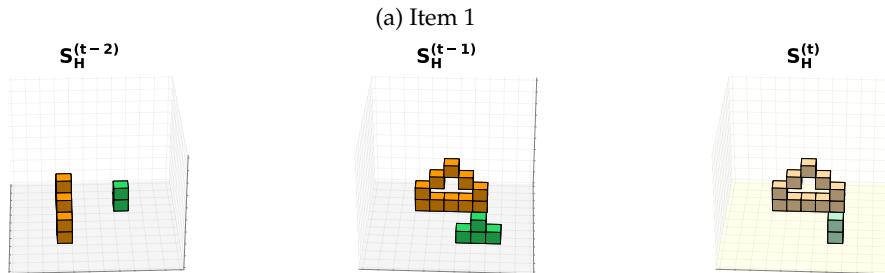
[B] wrow
 [A] Draw an orange 3x3 U on the ground

Figure 7: Empty board: Clear context with multiple interpretations and correct structure



[A] one orange tall on the three middle red
 [A] so dont stack them
 [B] oh, got you
 [B] horizontal?

[A] then put three orange on the side of the red



[A] now two green blocks on either side, paralell to the orange pyramid

[A] whoops, my bad

(b) Item 2

Figure 8: Unclear context

Fixing incorrect structures by looking ahead to the next correct structure. If the Builder made a mistake or their action sequence was interrupted by an utterance, the built

structure of a BAP item may be incorrect. E.g. in Figure 9a **B** places only one instead of two blocks. However, the next BAP item (Figure 9b) has a correct structure, and its structure is the one that should have been built in 9a because 9b completes the truncated action sequence. We can therefore replace the structure in 9a with the one in 9b. Figure 10 shows a sequence of three BAP items: in 10a **B** misinterprets **A** and makes an error, in 10b **B** realizes the mistake post **A**'s correction and proceeds to correct it, but **A** interrupts them, and in 10c, the mistake is finally rectified post the interruption. Items 10a and 10b with incorrect structures should therefore be amended to result in the correct structure built in 10c.

Manual analysis shows that sequences of one or more incorrect items (with clear contexts) that are immediately followed by a correct item (with clear context) can be fixed by replacing their built structures with the built structure of that subsequent correct item. Those items with incorrect structures that conform to this pattern are thus fixed automatically, and the remaining that can't are excluded from the final test set.

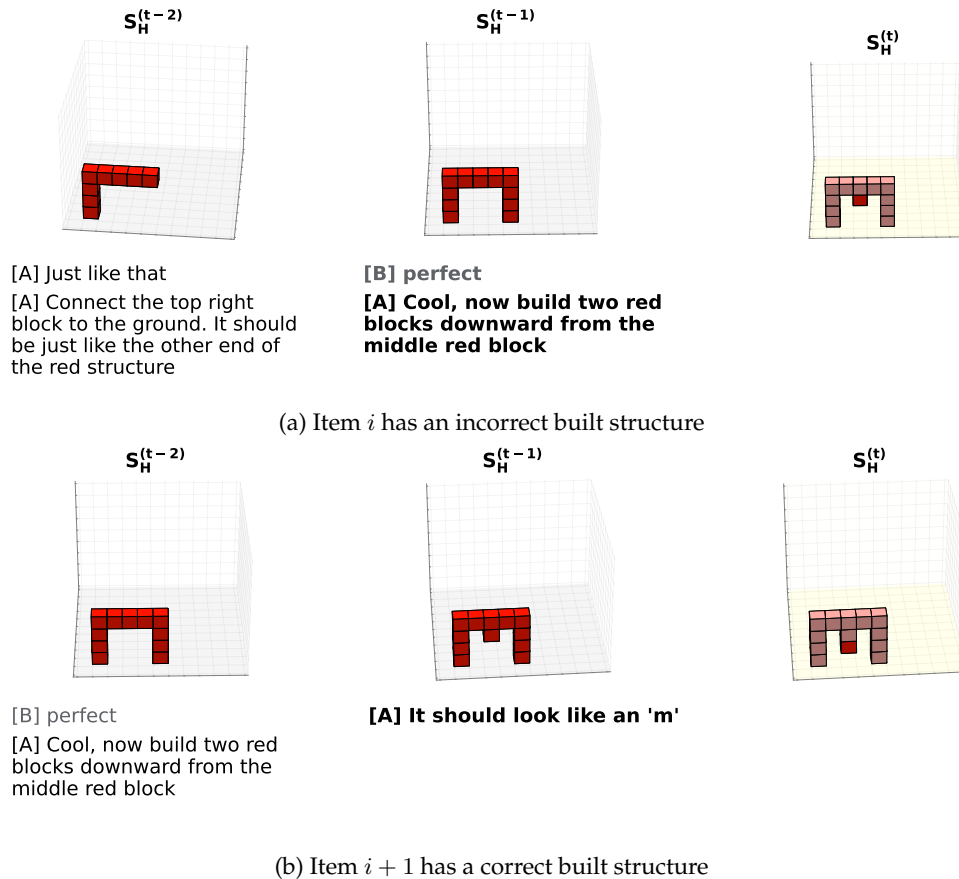
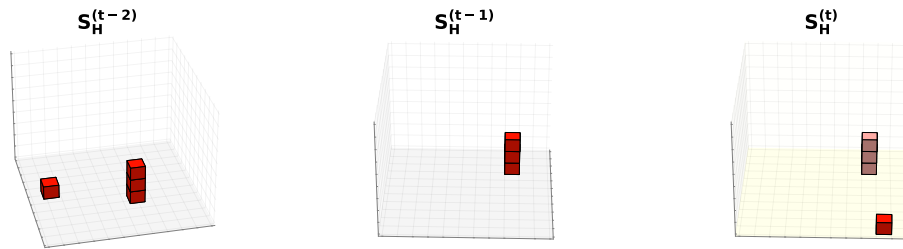


Figure 9: An item with an incorrect built structure (9a) that can be fixed by the correct built structure in the following item (9b)

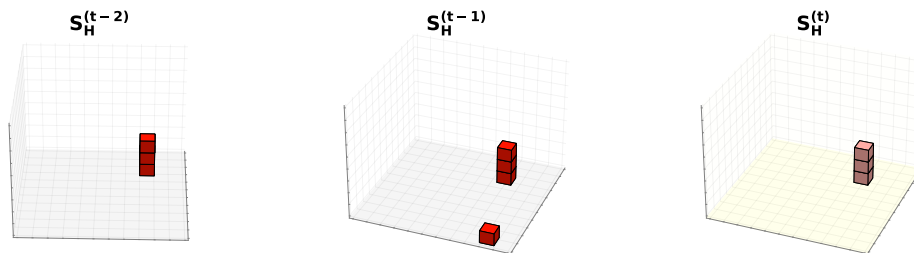
Statistics of the clean BAP v2 test set. The BAP v2 test set consists of **1,155 BAP items**, all of which have a **clear context** and a **correct built structure**. 1,071 of these items have



[A] so if you turn 90 degrees to your right, that might help with the perspective
 [A] Can you remove the brick you just added?

[A] Thanks!
[B] yeah sorry! but confusing
[B] bit*
[A] Ok, so if you turn to your right, that will help with the perspective a bit
[A] ok, so to the right of the top of that column, add two red bricks

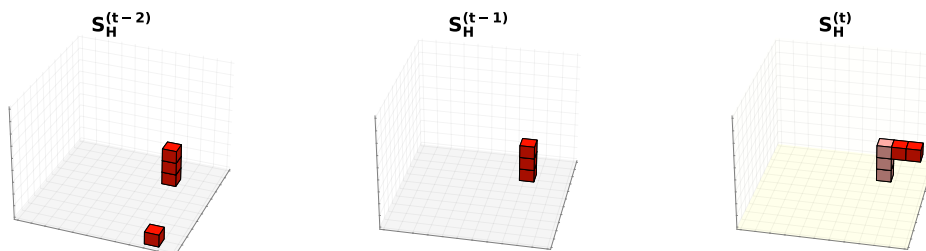
(a) Item i has an incorrect built structure



[A] Thanks!
 [B] yeah sorry! but confusing
 [B] bit*
 [A] Ok, so if you turn to your right, that will help with the perspective a bit
 [A] ok, so to the right of the top of that column, add two red bricks

[A] the column of red bricks

(b) Item $i + 1$ has an incorrect built structure



[A] the column of red bricks

[A] don't worry too much about the edge of the map stuff
[B] oh okay

(c) Item $i + 2$ has the correct built structure for items $i, i + 1$ and $i + 2$

Figure 10: A sequence of items with incorrect built structures (10a, 10b) that can be fixed by the following item's correct built structure (10c)

a unique correct interpretation, and 84 of the empty board (EB) items have multiple correct interpretations. This set was obtained from the original BAP test set of 1,616 BAP items by removing 461 items that should not be used for evaluation (418 with unclear contexts and 43 with incorrect structures that could not be fixed), and by fixing the structures of 149 items whose original structures were incorrect.

4. Revisiting BAP Evaluation: Metrics

We now revisit the strict F1 metric and propose a fairer variant that accounts for the fact that some EB items have multiple valid interpretations. Additionally, the current evaluation, relying solely on an aggregated F1 score, lacks detailed insights into model behavior. To address this, we introduce additional metrics. These contributions collectively define an updated **BAP v2 evaluation benchmark**.

4.1 Fairer F1

The clean v2 test set consists only of BAP items with a clear context and correct structures, but 84 of the EB items (7.3% of the v2 test set) do not have a unique interpretation, since their structure can be placed and oriented in many different ways (see Figure 7 above). The v2 test set can therefore be split up into items with a unique correct interpretation (\mathcal{U}) and items with multiple correct interpretations (\mathcal{M}). But while the strict F1 score defined in Section 2.4 is appropriate for items in \mathcal{U} , it unfairly penalizes Builders on items in \mathcal{M} when their structure is correct, but placed in a different location and/or orientation than the reference structure. A fair evaluation metric needs to account for these allowable changes in location and orientation for items in \mathcal{M} , i.e. structures placed on an empty board when the context does not uniquely identify their placement.

Recall from Section 2.3 that a structure $S = \{(\langle x, y, z \rangle, \mathbf{c})\}$ is a set of blocks that each have a color \mathbf{c} and a location $\langle x, y, z \rangle$, and that the distance $\Delta(S, S')$ between two structures S and S' is defined as the number of net actions of any action sequence that changes S to S' (or vice versa). To fairly compare two structures S, S' on the empty board, we first align them by searching for a translation \mathcal{A}_T^* of blocks in the horizontal plane and a rotation \mathcal{A}_R^* about the vertical axis in 90-degree intervals that transform S into a structure $S^* = \mathcal{A}_R^*(\mathcal{A}_T^*(S))$ in the BUILDREGION that is as close to S' as possible (i.e. where $\Delta(S^*, S')$ is minimized). We refer to the composed transform $\mathcal{A}_R \mathcal{A}_T$ as alignment \mathcal{A} , and call $\mathcal{A}^* = \arg \min_{\mathcal{A}} (\Delta(\mathcal{A}(S), S'))$ the optimal alignment of S to S' .

To evaluate a model’s net action set A_M^{net} against a human reference net action set A_H^{net} for an item in \mathcal{M} , where A_M leads from the (empty) board to a predicted structure S_M , and A_H leads from the (empty) board to a reference structure S_H , we therefore first identify an optimal alignment of the predicted structure to the reference, $\mathcal{A}^* = \arg \min_{\mathcal{A}} (\Delta(\mathcal{A}(S_M), S_H))$, and apply the same transformation \mathcal{A}^* to all actions in the model’s net action set A_M^{net} , yielding an aligned action sequence \tilde{A}_M^{net} that can now be fairly compared against A_H^{net} by our original strict F1 metric. That is, a **fairer F1 metric** computes a strict F1 score for the predicted action sequences A_M^{net} for any item in \mathcal{U} , because the reference sequences for these items yield the only correct structures for these items, but for any item in \mathcal{M} , it computes a strict F1 score for the optimally aligned predicted action sequences \tilde{A}_M^{net} because this item has multiple correct interpretations that only differ from each other in location and orientation. Thus, in the example in Figure 7, any predicted orange 3x3 U-shaped structure placed on the ground will receive a fairer F1 score of 1.0.

4.2 Auxiliary metrics

The current BAP evaluation relies solely on an aggregate F1 metric. While it reasonably reflects overall model performance (especially with fairer F1), it remains opaque and lacks detailed insight into specific model capabilities, such as spatial reasoning. This is a key missing aspect in the evaluation framework. To address this, we introduce finer-grained auxiliary metrics to complement the aggregate fairer F1 metric. These metrics aim to enhance evaluation robustness, provide deeper insight into model behavior, enable precise error analysis, better differentiate models, identify reasons behind a model’s performance changes, and ultimately guide the development of better models.

Type, Color, and Location F1. In analogy to the strict F1 score, we define auxiliary metrics that only evaluate certain aspects of the predicted actions. Recall that the strict evaluation assumes that a Builder action $a_M^m = (t, c, \langle x, y, z \rangle) \in A_M^{\text{net}}$ is correct if and only if there is an *equal* reference action $a_H^h = (t, c, \langle x, y, z \rangle) \in A_H^{\text{net}}$, and that our strict precision, recall and F1 scores are therefore based on the sizes of Builder and Human net actions and their intersection. To evaluate whether a Builder model correctly predicts action types t , colors c , or locations $\langle x, y, z \rangle$, we define corresponding evaluation metrics that consider Builder actions correct if and only if there is an *equivalent* reference action in A_H^{net} . We consider three different equivalence relations: **Type**, **Color** (and type), and **Location**:

Type equivalence: $(t, c, \langle x, y, z \rangle) \equiv_{\text{Type}} (t', c', \langle x', y', z' \rangle) \iff t = t'$

Color equivalence: $(t, c, \langle x, y, z \rangle) \equiv_{\text{Color}} (t', c', \langle x', y', z' \rangle) \iff t = t' \text{ and } c = c'$

Location equivalence: $(t, c, \langle x, y, z \rangle) \equiv_{\text{Loc}} (t', c', \langle x', y', z' \rangle) \iff \langle x, y, z \rangle = \langle x', y', z' \rangle$

(Note that the condition for Location equivalence is effectively the same as $t = t'$ and $\langle x, y, z \rangle = \langle x', y', z' \rangle$). Accordingly, we can transform both net action sets A_M^{net} and A_H^{net} into Type, Color or Location *multi-sets*:

$$M^{\text{Type}} = \{t \mid (t, c, \langle x, y, z \rangle) \in A^{\text{net}}\}$$

$$M^{\text{Color}} = \{(t, c) \mid (t, c, \langle x, y, z \rangle) \in A^{\text{net}}\}$$

$$M^{\text{Loc}} = \{\langle x, y, z \rangle \mid (t, c, \langle x, y, z \rangle) \in A^{\text{net}}\}$$

which yields Type, Color and Location (strict) precision, recall and F1 scores by comparing the sizes of the corresponding multisets and their intersections (we only show Type F1 below, as Color and Location F1 are similarly defined):

$$\text{Strict Type Precision } P_{\text{Type}}(A_M^{\text{net}}, A_H^{\text{net}}) = \frac{|(M_M^{\text{Type}} \cap M_H^{\text{Type}})|}{|M_M^{\text{Type}}|}$$

$$\text{Strict Type Recall } R_{\text{Type}}(A_M^{\text{net}}, A_H^{\text{net}}) = \frac{|(M_M^{\text{Type}} \cap M_H^{\text{Type}})|}{|M_H^{\text{Type}}|}$$

$$\text{Strict Type F1 } F1_{\text{Type}}(A_M^{\text{net}}, A_H^{\text{net}}) = \frac{2 \cdot P_{\text{Type}} \cdot R_{\text{Type}}}{P_{\text{Type}} + R_{\text{Type}}}$$

Intuitively, the Type F1 metric quantifies how good a model is at understanding what type of actions to perform – placements, or removals, or both, and how many of each type. The Color F1 metric narrows down Type F1 a bit more to factor for colors as well. It quantifies how good a model is at understanding the colors of blocks that need to be placed or removed. The Location F1 metric quantifies how good a model is at understanding the specific locations of blocks that need to be placed or removed (without regard to color), i.e., **spatial reasoning**. Also, as mentioned earlier, these metrics are analogous to the strict F1 metric. They can then be used to define their fairer counterparts in the same way the strict F1 was used to define the fairer F1. **Henceforth, we will use Type, Color and Location F1 to refer to their fairer counterparts.**

Shape F1. To evaluate how good a Builder model is at understanding the "shape" in which the required blocks need to be placed or removed, we define a metric, Shape F1, that is agnostic to the absolute $\langle x, y, z \rangle$ locations of the required blocks, but only cares that they be placed/removed in the right locations relative to each other. **Essentially, it compares net actions modulo their exact placement and orientation.** Therefore, similar to the methodology used for fairer F1 (Section 4.1), we optimally align the model's net actions A_M^{net} against the human reference net actions A_H^{net} (instead of the corresponding resulting built structures themselves like was done for fairer F1), yielding aligned net actions \hat{A}_M^{net} that can now be compared against A_H^{net} by our original strict F1 metric. This is done for all items in the v2 test set (and not just the ones with multiple interpretations like was done for fairer F1). We will see examples of Shape F1 and the other auxiliary metrics later in Sections 7.2 and 8.1.

4.3 Micro vs Macro F1

Current BAP evaluation reports the micro-averaged F1 (micro F1) over all action sequences in the test data (Section 2.4), reflecting a model's quality in predicting individual actions. However, since the BAP task requires sequence prediction, it's equally important to assess the model's quality in predicting entire action sequences using the macro-averaged F1 (macro F1). Intuitively, this is also particularly relevant for Shape F1, which measures the model's performance on a broader sequence-level property (the "shape" of the net actions). Therefore, hereafter, we will report both micro and macro F1.

4.4 BAP v2 evaluation benchmark

The above metrics enable a fairer, robust, and more insightful evaluation on the clean v2 test set. We use the fairer F1 metric to report both micro and macro F1 scores in Tables 1 and 2 respectively. For each, we include both auxiliary and overall F1 metrics, and report them on the overall/full test set and separately for the EB and NEB subsets as well. This forms the **BAP v2 evaluation benchmark**. Our approach also enables more accurate evaluation within the EB and NEB categories, offering a clearer understanding of model performance across these two distinct scenarios. This division is important for the following reasons:

- EB examples are generally the easiest for the BAP task, making EB performance a basic competency or sanity test, and it also reflects a model's maximum potential quality.

- EB performance is also an estimate of the ability of a model to begin a game accurately – an elementary yet important trait to measure. Moreover, in an interactive/online setting, from a user (human Architect) experience perspective and considering the potential for subsequent cascading errors, mistakes made in EB scenarios can potentially be costlier than those in NEB, as EB marks the start of a game (even though EB examples in the data are far fewer than NEB). Quantifying EB performance will help provide a sense for how a model can potentially fare in an interactive setting wrt this aspect.

We begin with the micro scores in Table 1 for direct comparison with our prior work. Recall that the baseline model achieves an F1 score of 21.1% under the strict F1 metric. This increases to 27.3% under the fairer F1 metric (the overall F1 on the overall dataset), **a notable difference of 6.2 percentage points and a 29.4% improvement**. This highlights the **importance of the high quality cleaner test data and the fairer F1 metric in providing a fairer reflection of model capability**. On the overall dataset, the model achieves reasonably good F1 scores of 65.2% for Type and 62.4% for Color, but only 27.7% for Location F1, which is also very close to the overall F1 of 27.3%. This suggests that **spatial reasoning (Location F1) is the key bottleneck for high performance on this task**. As expected, the model performs better on EB than NEB across all metrics. Recall that the number of EB items are fewer than NEB items though (and the metrics on the overall dataset will therefore be more influenced by NEB). Next, we turn to the macro scores in Table 2. While all values increase compared to the micro scores, the overall trends remain the same. The overall F1 on the overall test set increases from 27.3% (micro) to 28.1% (macro). The model achieves a Shape F1 of 36.3% (micro) and 41.1% (macro) on the overall test set, with the macro score providing a more intuitive measure in this context, as discussed in Section 4.3.

Hereafter, we will use the v2 evaluation to report model performance.

Dataset	Type	Color	Location	Shape	Overall
EB	76.4	75.2	53.5	56.0	53.2
NEB	63.8	60.8	24.6	33.8	24.2
Overall	65.2	62.4	27.7	36.3	27.3

Table 1: Micro F1 scores for the baseline model under the v2 benchmark

Dataset	Type	Color	Location	Shape	Overall
EB	80.9	79.8	61.5	64.9	61.2
NEB	73.1	69.9	25.7	39.0	25.2
Overall	73.8	70.7	28.5	41.1	28.1

Table 2: Macro F1 scores for the baseline model under the v2 benchmark

5. Revisiting BAP Data: Generating Synthetic Data

One key challenge of the BAP task is the limited training data, despite the data augmentation (Section 2.5). We aim to avoid simply collecting more data like the MDC, due to scalability issues and the desire to stay aligned with many realistic scenarios, where data collection for complex situated dialogue tasks, like the MCBT, can be impractical/expensive, warranting exploration of alternative methods. Additionally, we observe that the baseline model struggles primarily with spatial reasoning, as reflected in its Location F1 score. These reasons motivate the need for additional synthetic training data that, while naturally simpler than the MDC, remains rich in spatial relations and referential expressions to help train more robust models. Looking ahead, such data could also be crucial for training more sophisticated, data-hungry deep transformer models and training/fine-tuning increasingly large LLMs. (We, in fact, also illustrate the impact of this data on training a simple LLM and transformer-based model in Section 6.3.)

We design **novel Minecraft dialogue and target structure simulators** that emulate the MCBT, and use them to generate a set of three synthetic dialog datasets with corresponding target structures. Each dataset is modeled after the MDC and is understandably simpler, while preserving essential elements of realistic human behavior observed in the MDC as much as possible, such as the language, clarification exchanges, Architect **A**'s and Builder **B**'s planning perspectives, dialog flow, etc. Across these datasets, we vary the level of instruction abstraction, the complexity of spatial relations and referential expressions, the complexity of target structures, etc. Special emphasis is laid on spatial relations as that is a core part of our motivation here. Each dataset is thus unique, contributing to the overall diversity and richness of the overall set.

Note that although our primary focus is on BAP, the simulators and data introduced here are applicable to other MCBT subtasks as well (e.g. the AUG subtask; Section 2.1.2), supporting advancements across the broader MCBT ecosystem. We discuss this in more detail in Section 8.4.

5.1 General dialog simulation framework

5.1.1 Desiderata. Similar to the target structures and game logs in the MDC, the following components of synthetic dialogues need to be generated:

- The target structure
- The dialogue/game – a chronological sequence that interleaves the following elements:
 - A dialogue between **A** and **B**, consisting of utterances that include instructions, potential clarification exchanges, etc.
 - **B**'s position and orientation at appropriate points in the game, i.e., when an utterance or action is recorded (Grounded elements of the dialog, e.g. spatial relations, are always wrt this frame of reference.)
 - **B**'s actions, which reflect the evolving structure being built

5.1.2 High-level Algorithm. As described in Section 2.1, the MCBT task is asynchronous and loosely structured. The MDC dialogs are real human-human game logs collected in a low-stakes, free-flowing setting with minimal constraints on participants' language and actions. To enable tractable simulation and facilitate simpler synthetic data generation, we make some simplifications and structure the task as follows.

Our dialog simulators generate synthetic dialogs that meet the desiderata, following a general framework. At a high level, it is an iterative procedure that continues until the target structure is built. The target structure may be provided as input or generated dynamically. In the former case, a separate simulator generates target structures. Each iteration produces one dialog segment—**A**'s instruction followed by **B**'s actions in response, with optional clarification exchanges and confirmations—leading to the construction of a part of the target structure. We are essentially simulating **A** and **B**, including their latent planning processes. Each iteration proceeds as shown below. (We use Figure 11 as an example. It illustrates a BAP item $(\mathcal{H}^{t-1}, S^{t-1}, D^t, A^t, S^t)$ from one of our synthetic datasets (recall notation from Section 2.2). In this iteration, the dialog and actions following S^{t-1} are simulated to produce the next structure, S^t – specifically, simulating D^t , A^t , and S^t .)

1. **Architect Planning:** First, **A**'s plan for the next steps is simulated, including which blocks to place or remove and their order if multiple blocks are involved. A reference block is chosen when necessary, enabling **A** to describe the new block(s) with appropriate spatial relations wrt the reference block. E.g., in Figure 11, **A** decides to place the red floating block, using the previously placed blue block as the reference.
2. **Builder Position and Orientation:** A "valid" position and orientation for **B** is sampled, ensuring a frame of reference for the utterances in the dialog segment. **B** is positioned at a suitable distance from the action area and oriented to face it while adhering to world constraints. E.g., in Figure 11, the structure S^{t-1} is rotated according to **B**'s gaze (yaw angle only).⁴
3. **Architect Instruction:** An instruction from **A** is synthesized, incorporating necessary block details (e.g. color), spatial relations, and referential expressions, with template-based lexical and syntactic variations. E.g., in Figure 11, **A** instructs, "put a floating block ...".
4. **Optional Clarification Exchange:** Some information may be omitted from the instruction with a small probability, allowing **B** to ask a clarification question. An appropriate exchange is then generated, with **B** asking and **A** providing the missing information. E.g., in Figure 11, the block's color is omitted, prompting **B** to ask, "what color?" and **A** to reply, "red".
5. **Builder Actions and Low-Level Planning:** **B**'s actions to add/remove blocks are then simulated, including any necessary low-level planning for deciding order of actions and accounting for temporary supporting blocks. This updates the built structure. E.g., in Figure 11, **B** places the red floating block to produce structure S^t , temporarily adding/removing support for the floating block.⁵
6. **Optional Confirmation from Builder:** Optionally, a confirmatory utterance from **B**, like "done," may be synthesized with a small probability.

We implement this general framework in three distinct ways, resulting in three different simulators. Each simulator uniquely instantiates steps 1, 3, and 4, along with

⁴ **B**'s position and pitch angle is omitted in our figures for clarity as noted in Section 2.2

⁵ Temporary supporting blocks are not shown in our figures as noted in Section 2.2.

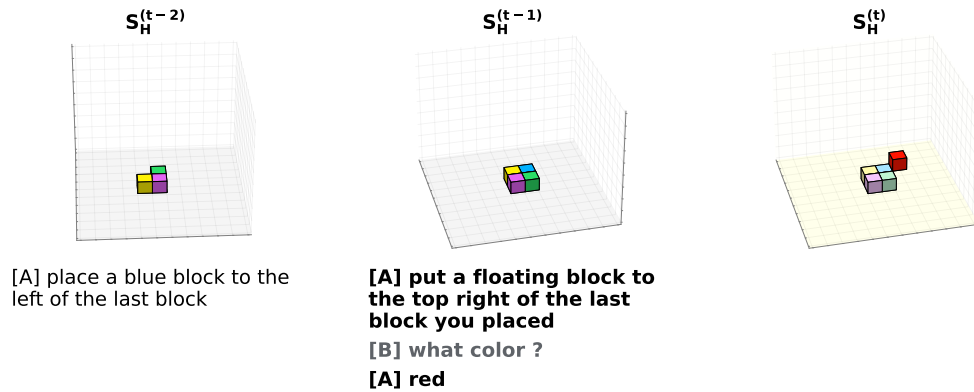


Figure 11: A BAP item from one of our synthetic datasets

independent target structure generation, while steps 2, 5, and 6 remain largely consistent across simulators. For brevity, we provide only a summary of each simulator in the following sections, with detailed descriptions in the appendix.

5.1.3 Spatial Relations. Given the special emphasis on spatial relations in our dataset design, we briefly outline them here. We focus on the following types of spatial relations:

1. **Relative to a Reference Block:** We can describe the location of a target block in relation to another block, referred to as the reference block. Around the reference block, there are 6 rows, 12 quadrants, and 8 octants where the target block may be positioned. This leads to the following spatial relations (all of them are considered with respect to **B**'s POV/frame of reference):
 - (a) **1D:** The target block lies in one of the rows, differing from the reference block in only one dimension. This results in 6 basic spatial relations: left, right, top, bottom, front, and behind (e.g., "to the right of ...", "behind ...").
 - (b) **2D:** The target block lies in one of the quadrants, differing in exactly two dimensions. This results in 12 possible combinations of the 1D relations, such as top+right, bottom+left, etc. (e.g., "to the top right of ...").
 - (c) **3D:** The target block lies in one of the octants, differing in all three dimensions. This results in 8 possible combinations of the 1D relations, such as top+right+front (e.g., "one to the left, one above, and one block behind ...").

These 1D/2D/3D relations apply when one needs to specify spatial relations between blocks or substructures/shapes.
2. **Using **B** as a Spatial Anchor:** Spatial relations can also be described using **B** as a spatial anchor directly (e.g., "going up and to the left of you"). These only apply when one needs to specify the direction in which to build a certain substructure/shape, e.g., a diagonal.

We will see concrete examples of these in the following sections.

5.2 Random target structures and dialogs

Dialogs. The dialogs correspond to random target structures generated dynamically during the dialog simulation (Section 5.1.2) which runs for a maximum number of iterations. Blocks are placed/removed randomly, and one at a time in each iteration, with limited planning on A's part for block placement. As a result, the target structure is disordered, and A's instructions are fairly low-level, addressing only one block at a time. Most of them use spatial relations relative to arbitrary blocks identified by color and location (e.g., "to the right of the red" or "to the right of the bottom-most red block"). Figure 12 shows an example BAP item from this dataset. A identifies the orange block as a reference block and uses a 1D spatial relation "behind" to specify the target yellow block.

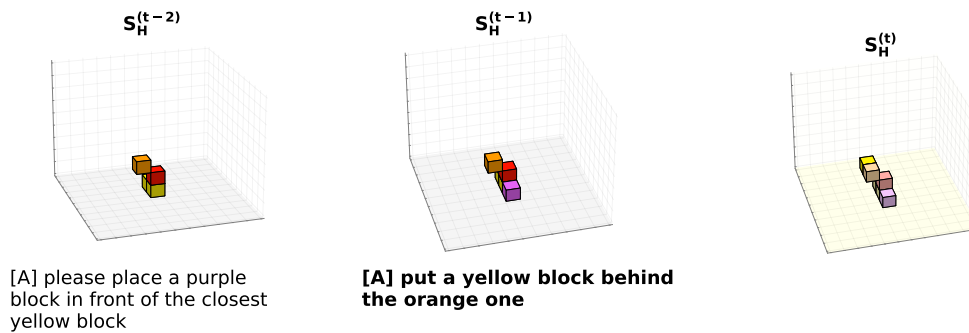


Figure 12: A BAP item from the random structure-based dialogs

Target structures. Target structures are generated dynamically during the dialog simulation and correspond to the final built structure at the simulation's end. Some global constraints are enforced:

1. The structure must have at least one block on the ground.
2. The entire structure must be "connected," i.e., each block shares at least one face or edge with at least one other block.

Figure 13 provides an example.

5.3 Shape-based target structures and dialogs

Target structures in the MDC are not random; they are far more ordered (e.g., a dining table) and often composed of meaningful shapes/concepts (e.g., rows, towers, diagonals, planes, etc.). Architect instructions describe these structures at various levels of abstraction, from high-level references to the whole structure ("flower" or "bell tower"), mid-level references to sub-shapes ("row" or "plane"), down to low-level instructions referencing individual blocks. This observation motivates the need for similarly structured synthetic data as well. We first describe a simulator that can generate these

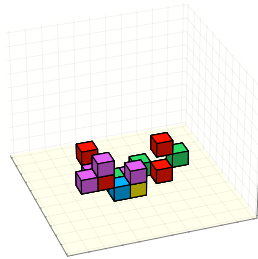


Figure 13: A random target structure

structures (Section 5.3.1), and then outline two types of dialogs simulated based on these structures (Sections 5.3.2 and 5.3.3).

5.3.1 Shape-based structures. We define six unique elementary 3D shapes: **rows, diagonals, T-shapes, L-shapes, U-shapes, and planes**. These shapes were chosen for their simplicity and occurrence in MDC dialogs and structures. Formal definitions of these shapes are provided in the appendix. We design a simulator that generates target structures by combining multiple randomly sampled elementary shapes into a single composite structure. Sampling is performed with replacement, allowing multiple instances of the same shape type within a structure. For each shape instance, properties such as size, color, orientation, and exact 3D location are randomly sampled within specific constraints (e.g., minimum and maximum size bounds). Some global constraints are also enforced (similar to those for random structures in Section 5.2, with an added constraint for shapes):

1. The structure (i.e. at least one shape) must have at least one block on the ground.
2. The entire structure must be "connected", i.e., each block shares at least one face or edge with at least one other block, and each shape instance shares at least one block face or edge with at least one other shape instance.

The simulator is flexible, allowing parameters such as shape types, number of shapes per structure, etc. to be customized. Figure 14 illustrates two examples of such target structures.

5.3.2 Blocks-based dialogs for shape-based structures.

Target structures. Each target structure consists of three shape instances, sampled from the full set of the six elementary shapes.

Dialogs. The dialog simulation (Section 5.1.2) takes the target structure as input and continues iteratively until the target structure is built. Construction proceeds one shape at a time. **A**'s planning is involved and follows a heuristic that selects one or more blocks to place in each iteration until all shapes are completed. Consequently, **A**'s instructions reference a single block or multiple ones collectively, with each shape decomposed into

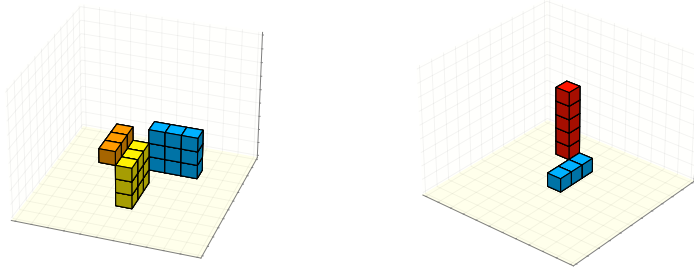


Figure 14: Shaped-based target structures

multiple instructions. Most of **A**'s instructions include spatial relations relative to the last block placed by **B** (e.g., "now, place two red blocks behind the last block"). Figure 15 illustrates an example BAP item from this dataset. The first blue square has been built, and the second (yellow) shape is under construction. **A** is instructing **B** to continue building the latter by placing three more blocks, using a 1D spatial relation "on top of" relative to the last block. (In the previous step, **A** used a 2D spatial relation, "diagonally in front of and to the right of".)

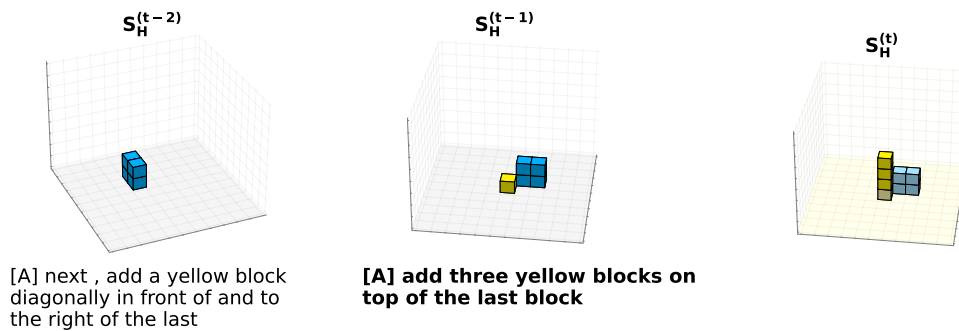


Figure 15: A BAP item from the blocks-based dialogs for shape-based structures

5.3.3 Shape-based dialogs for shape-based structures.

Target structures. For tractability in dialog simulation and to prevent overly complex utterances, each target structure is limited to two shape instances, sampled from only three elementary shapes: rows, diagonals, and planes.

Dialogs. The dialog simulation (Section 5.1.2) takes the target structure as input and proceeds shape by shape, with one complete shape placed per iteration until the target is built. **A**'s planning employs simple heuristics to determine the order of shapes and select a target block within each shape for defining spatial relations, which also serves as **B**'s starting point for building the shape. **A**'s instructions, therefore, describe entire

shapes rather than individual blocks, resulting in higher-level, abstractive instructions. Since each target structure consists of two shapes, each placed in one go, a 1D/2D/3D spatial relation is only used to specify the position of the initial block of the second shape relative to the last block placed in the first shape. Additionally, **A** can also use spatial relations that use **B** as a spatial anchor (Section 5.1.3), for building either shape. Figure 16 illustrates a BAP item from this dataset. The first shape (a yellow column) has been built, and **A** is instructing **B** to build the second shape (a red row) in one go. **A** uses the spatial relation "going to the left of you" (using **B** as a spatial anchor) to indicate the direction for the row, along with the 3D spatial relation "one to the left, two underneath, and one block in front of" relative to the last block (the topmost yellow one), to indicate the starting position for the row.

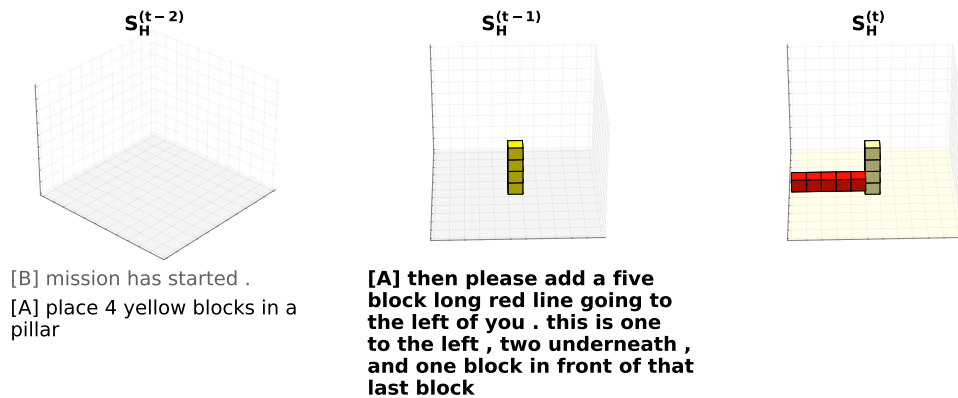


Figure 16: A BAP item from the shapes-based dialogs for shape-based structures

6. Training with Synthetic Data

Our next objective is to demonstrate that the synthetic data can help train much better models for the BAP task, even with simple training methods, thereby addressing the challenge of insufficient training data. We first show that simple joint training on the aggregation of the synthetic data and the original BAP (augmented) data already yields a better model (Section 6.1). We then go a step further and show that a simple Curriculum Learning method can further boost performance (Section 6.2). The synthetic data together with the original BAP (augmented) data now constitutes the **BAP v2 training dataset**, completing the BAP v2 framework. We also illustrate the impact of the synthetic data and training methodologies on training a simple LLM (BERT) and transformer-based model (Section 6.3).

A note on experimental design choices. For the GRU-based models in Sections 6.1 and 6.2, we maintain the same architecture and hyperparameters as the baseline model (Section 2.6), along with the same amount of data augmentation in the BAP training data as in our prior work (Section 2.5). Fine-tuning these aspects for different training methods is beyond the scope of our objectives here and left for future work to further optimize performance. Similar choices made for the BERT-based models are discussed later in Section 6.3.

Key Terminology. Hereafter, we refer to the random structure-based dialogs (Section 5.2) as D_r , blocks-based dialogs for shape-based structures (Section 5.3.2) as D_{bs} , and shape-based dialogs for shape-based structures (Section 5.3.3) as D_{ss} . The Minecraft-based original BAP data is denoted as D_{mc} . Each dataset includes train, test, and val splits, with the D_{mc} train set also incorporating augmented data from Section 2.5. The baseline model (Section 2.6), trained on D_{mc} alone, is denoted as M_{mc} .

6.1 Joint training on aggregated data

The most straightforward approach to use the synthetic datasets (D_{bs} , D_{ss} , D_r) is to just combine them all together along with the original D_{mc} data and retrain the baseline model on this aggregated dataset.

6.1.1 Experimental Setup. Our setup closely follows that of Section 2.6, where the baseline M_{mc} was trained on D_{mc} alone. We retain the same exact model architecture and hyperparameters as in M_{mc} . Training employs teacher forcing with cross-entropy loss, and decoding is performed via greedy decoding, with a maximum sequence length of 20 actions. We use the fairer F1 metric to report micro F1 scores on the BAP v2 test set for D_{mc} (Section 4.4) and the test sets of D_{bs} , D_{ss} , D_r .⁶ Results on the full v2 evaluation benchmark are reported for the baseline and best performing models in this work later in Section 7.1.

How much of each synthetic dataset to use during train time? An important consideration is determining the optimal amount of each synthetic dataset to use alongside D_{mc} in the training dataset. We adopt an empirical yet systematic approach to address this, yielding a data mix that optimizes D_{mc} performance while also being highly performant on the synthetic data as much as possible. Details can be found in the appendix. Table 3 presents the final data statistics. Similar to the methodology used for data splits for the MDC (Narayan-Chen, Jayannavar, and Hockenmaier 2019), for each of the synthetic datasets, the game logs are split into disjoint test, training, and validation sets such that training target structures do not appear during test or validation. We now have a total of 52419 items in the aggregated training dataset.

Dataset	Train	Val	Test
D_{bs}	9890	1186	1181
D_{ss}	11868	1000	1000
D_r	15825	1161	1089
D_{mc}	14836	1331	1616

Table 3: Data statistics (#items) for training, validation, and test splits across datasets.

6.1.2 Experiments and Results. Table 4 presents the results. We denote the model trained on the aggregated dataset as M_{agg} , and include comparisons to the baseline model (M_{mc} – trained on D_{mc}), and models trained on the three synthetic datasets separately (M_{bs} , M_{ss} , M_r – trained on D_{bs} , D_{ss} , D_r respectively). F1 performance is

⁶ For fairer F1 on D_{bs} , D_{ss} , D_r , \mathcal{M} consists of all EB items, unlike D_{mc} , where only a subset is considered (Section 4.1). This is because, by design, all EB items in D_{bs} , D_{ss} , D_r have multiple correct interpretations.

reported (as percentages) on the respective test sets of all four datasets (D_{bs} , D_{ss} , D_r , D_{mc}).

M_{agg} achieves an F1 score of 30.3% on D_{mc} , up from the baseline model M_{mc} 's 27.3%, **a notable 3-percentage point improvement**. Additionally, M_{agg} is **highly performant across the synthetic datasets** (D_{bs} , D_{ss} , D_r), surpassing M_{mc} by large margins on these. For a sense of what high performance means on these datasets, we reference the diagonal entries in rows for models M_{bs} , M_{ss} , M_r , representing performance of these models on the same test data distribution as train: 83.9% for D_{bs} , 75.4% for D_{ss} , and 64.4% for D_r . In light of these numbers, **the baseline M_{mc} underperforms significantly on the synthetic datasets, despite being trained on the far more complex D_{mc} data**; it even performs worse on datasets D_{ss} and D_r than on D_{mc} . In contrast, M_{agg} is more robust, and retains much of the diagonal-entry performance on the synthetic datasets while also significantly improving on D_{mc} . It is also better on the synthetic datasets than on D_{mc} by large margins (as it should be), unlike M_{mc} . Lastly, the models trained solely on synthetic datasets perform poorly on D_{mc} , as does M_{mc} on synthetic data, indicating that **joint training on the aggregated dataset is essential for robust performance** across both real and synthetic data.

Model	Train Data	Test Data			
		D_{bs}	D_{ss}	D_r	D_{mc}
M_{mc}	D_{mc}	35.2	19.1	12.4	27.3
M_{bs}	D_{bs}	83.9	12.9	44.9	6.3
M_{ss}	D_{ss}	11.3	75.4	7.9	9.1
M_r	D_r	43.8	10.1	64.4	7.7
M_{agg}	$D_{bs}, D_{ss}, D_r, D_{mc}$	83.4	68.8	63.6	30.3

Table 4: Models trained on datasets separately (M_{mc} , M_{bs} , M_{ss} , M_r) and together (M_{agg})

6.2 Curriculum Learning (CL)

Another key observation from Table 4 is that performance of the M_{bs} , M_{ss} , M_r , and M_{mc} models decreases in the order $M_{bs} > M_{ss} > M_r > M_{mc}$, suggesting that the complexity/difficulty of examples increases in the order $D_{bs} < D_{ss} < D_r < D_{mc}$, with the most complex D_{mc} examples naturally appearing at the end. This observation raises the possibility of using this ordering to improve over the simple joint training approach (where data is randomly ordered) when training on the aggregated dataset, so as to achieve even better performance on the complex D_{mc} . Curriculum Learning (CL) is a natural next step to explore in this direction. CL is a training strategy that sequences training data from simpler to more complex examples, similar to human learning. Introduced by Bengio et al. (2009), CL begins with easier examples, gradually increasing in difficulty. This progression allows the model to first learn basic patterns and representations, building a foundation before tackling more challenging cases, which can enhance generalization and improve performance on complex tasks.

6.2.1 CL Mechanics.

Difficulty Metrics. A key prerequisite in CL is establishing difficulty metric(s) that quantify how difficult a training example is for a model to learn, allowing the data to be sorted accordingly during training. In this work, we explore three simple, natural, and intuitive difficulty metrics, along with their combinations (e.g., sorting first by one metric and then sorting (breaking ties) by another). The first metric is the **dataset** D an example belongs to (D_{bs} , D_{ss} , D_r , D_{mc}). As mentioned before, the datasets can be ordered as $D_{bs} < D_{ss} < D_r < D_{mc}$ in terms of difficulty. Additionally, we consider the lengths of the action (output) and input sequences: the **action (output) sequence length** L_A reflects the number of actions in the gold action sequence, while the **input sequence length** L_I measures the number of tokens in the game history fed to the model. These are also intuitive as longer sequences are harder to generate as output and process as input.

CL Algorithm. We make use of a simple CL algorithm, specifically using the Curriculum Arrangement algorithm within the CL framework proposed by Xu et al. (2020). Details of the method are provided in the appendix.

6.2.2 Experiments and Results. Overall experimental setup remains similar to the batch training one (Section 6.1.1). We experiment with each of the three difficulty metrics individually and the four possible combinations of them, making a total of seven metrics – D , L_A , L_I , (D, L_A) , (D, L_I) , (L_I, L_A) , and (D, L_I, L_A) (ordering within a tuple denotes the sorting order). We also experiment with the CL algorithm’s hyperparameter, N , trying six values – 5, 10, 15, 20, 25, and 30. (This controls the number of buckets/difficulty levels – see appendix.) This results in a grid of $7 \times 6 = 42$ experiments.

Table 5 presents the best model, M_{agg+cl} , selected based on D_{mc} performance. For comparison, we also include the baseline M_{mc} , and the aforementioned M_{agg} model (Table 4). On D_{mc} , M_{agg+cl} achieves an F1 of 33.0%, **a notable 2.7-point improvement over M_{agg} , and an even more significant 5.7-point improvement over the baseline M_{mc} .** It also continues to be highly performant on the synthetic data similar to M_{agg} . Thus, **Curriculum Learning on the aggregated data provides a meaningful performance boost** on the BAP task over simple joint training. Hereafter, we refer to M_{agg+cl} as the **best model**.

Model	Train Data	Test Data			
		D_{bs}	D_{ss}	D_r	D_{mc}
M_{mc}	D_{mc}	35.2	19.1	12.4	27.3
M_{agg}	$D_{bs}, D_{ss}, D_r, D_{mc}$	83.4	68.8	63.6	30.3
M_{agg+cl}	$D_{bs}, D_{ss}, D_r, D_{mc}$	84.0	68.8	60.3	33.0

Table 5: Curriculum learning (M_{agg+cl}) compared to models M_{mc} and M_{agg}

6.3 Transformers and LLMs (BERT)

As noted in Section 1, modeling is not the primary focus of this work. However, solely to test the robustness of our synthetic data and training methodologies and show their applicability to relatively contemporary model architectures, we experiment with a very simple alternative version of the baseline model (Section 2.6) that incorporates a

Transformer architecture (Vaswani et al. 2017) and an LLM (BERT; Devlin et al. (2019)). Specifically, we replace the GRU-based encoder (and GloVe embeddings) with BERT and substitute the GRU decoder with a Transformer, keeping the rest of the architecture unchanged (Figure 4). (A projection layer is added atop BERT for dimensionality reduction.) The simplicity also allows us to assess whether/to what extent simpler LLMs like BERT and vanilla Transformers alone can already effectively handle the BAP task. Future work can build on the insights we obtain to explore more sophisticated LLMs and architectures while leveraging the BAP v2 framework.

Model details. To control the representation dimensionality and complexity of the decoder transformer, we add a simple feedforward projection layer atop BERT, compressing its output (as otherwise the dimensionality of the decoder transformer would be forced to be the same as the BERT encoder and make it overly complex than need be). The BERT encoder and transformer decoder are connected in standard encoder-decoder fashion but via the projection layer. BERT’s token embeddings are compressed by the projection layer, and the transformer decoder then attends to these representations at each decoding time-step, and the representation dimensionality of the decoder matches the output size of the projection layer. This also matches the embedding dimensionality for action vectors fed into the decoder. Positional embeddings are also used for the decoder input. The output of the decoder’s last layer conditions the CNN-based action predictor (replacing the GRU hidden state from the baseline model).

6.3.1 Experiments and Results. We conduct similar experiments with this model like with the GRU-based model, i.e., training on D_{mc} only, joint training on the aggregated dataset, and CL. The experimental setup and the CL experiments are same as before (Sections 6.1.1 and 6.2.2). We tested various sizes of BERT models (Turc et al. 2019), keeping BERT frozen, and found that BERT_{BASE} (110.1M parameters) performed best. In the transformer decoder, five layers yielded optimal results, and a projection layer output size of 256 proved most effective. For tractability of experimentation, we only experimented with the number of transformer layers and the projection layer’s output size, keeping other architectural hyperparameters identical to the GRU-based models. Details specific to training regime, corresponding hyperparameters, etc. can be found in the appendix. Results are shown in Table 6. (*Note: We also experimented with finetuning BERT, but found the frozen scenario to perform relatively better. However, as with the frozen case below, synthetic data and CL improved performance in the finetuning scenario as well, demonstrating the robustness of our approach. Results are provided in the appendix.*)

Robustness of our approach. Overall trends align with those observed for the GRU-based models in Table 5. The synthetic data, joint training on the aggregated dataset, and CL, all also improve the BERT-based model’s performance on both synthetic and real data, highlighting the **robustness of our approach**. M'_{agg} achieves an F1 score of 29.4% on D_{mc} , up from M'_{mc} ’s 23.0%, **a notable 6.4-percentage point improvement**. It is also **highly performant across the synthetic datasets** (D_{bs} , D_{ss} , D_r), surpassing M'_{mc} by large margins on these. On D_{mc} , CL again yields the best-performing model, as with the GRU-based models. M'_{agg+cl} achieves an F1 of 32.3%, **a notable 2.9-point improvement over M'_{agg} , and an even more significant 9.3-point improvement over M'_{mc}** . It also achieves significant gains in performance over M'_{agg} on the synthetic data as well.

Comparison to GRU-based models. The lower performance of the BERT-based models than their respective GRU-based counterparts’ is more pronounced for performance on the

synthetic data than the Minecraft D_{mc} data. M'_{mc} achieves an F1 of 23.0% on D_{mc} , 4.3 points lower than M_{mc} 's 27.3%. This gap between the GRU-based and BERT-based counterparts reduces significantly as we move on to look at M'_{agg} and M'_{agg+cl} . It goes down to 0.9 and 0.7 points respectively. M'_{agg+cl} is therefore not too far below M_{agg+cl} . The gap in synthetic data performance between M'_{agg} and M_{agg} is fairly significant. But CL reduces this quite a bit – M'_{agg+cl} is very close to M_{agg+cl} on D_{ss} , although still behind on the other two. Two key factors contribute to the relatively lower performance of the BERT-based models compared to their GRU counterparts:

- As mentioned earlier, the sizes of all four datasets were optimized for the GRU-based models. These might need separate tuning for the BERT-based models (and will probably need to be scaled up also as transformers are more complex and data-hungry than GRUs).
- For tractability of experimentation, we only experimented with the number of transformer layers and the projection layer's output size, keeping other architectural hyperparameters identical to the GRU-based models.

These choices were intentional, as our goal here (as stated in the beginning of this section) was primarily to demonstrate the robustness of our synthetic data and training approach, and not to optimize dataset sizes or architectural hyperparameters for maximizing performance. We leave such fine-tuning for future work.

Model	Train Data	Test Data			
		D_{bs}	D_{ss}	D_r	D_{mc}
M'_{mc}	D_{mc}	29.1	17.8	12.0	23.0
M'_{agg}	$D_{bs}, D_{ss}, D_r, D_{mc}$	70.2	55.0	36.8	29.4
M'_{agg+cl}	$D_{bs}, D_{ss}, D_r, D_{mc}$	75.9	67.4	45.3	32.3

Table 6: BERT- and transformer-based models

7. Model Analysis

We now analyze the performance and behavior of the best model M_{agg+cl} (Section 6.2.2) relative to the baseline M_{mc} (Section 2.6). In Section 7.1, we do so using the BAP v2 evaluation benchmark introduced in Section 4.4. Section 7.2 complements this with a qualitative evaluation of outputs from both models.

7.1 Quantitative evaluation

Tables 7 and 8 present all metrics obtained using the v2 benchmark, augmenting Tables 1 and 2 (Section 4.4) with results for the best model. **Overall, the best model outperforms the baseline across all metrics.** Key takeaways are discussed below.

We begin with the micro scores in Table 7. On the overall dataset, the best model outperforms the baseline on all three F1 metrics: Type, Color, and Location. As noted in Section 4.4, Location F1 is the primary bottleneck to achieving high performance in this task. The best model achieves an overall F1 of 33%, a notable 5.7 percentage-

Dataset	Model	Type	Color	Location	Shape	Overall
EB	Baseline (M_{mc})	76.4	75.2	53.5	56.0	53.2
	Best (M_{agg+cl})	81.4	80.0	61.8	65.5	61.6
NEB	Baseline (M_{mc})	63.8	60.8	24.6	33.8	24.2
	Best (M_{agg+cl})	66.0	63.2	30.2	39.4	29.6
Overall	Baseline (M_{mc})	65.2	62.4	27.7	36.3	27.3
	Best (M_{agg+cl})	67.7	65.0	33.6	42.2	33.0

Table 7: Micro F1 scores for the baseline and best models under the v2 benchmark

Dataset	Model	Type	Color	Location	Shape	Overall
EB	Baseline (M_{mc})	80.9	79.8	61.5	64.9	61.2
	Best (M_{agg+cl})	83.1	81.7	69.0	72.6	68.6
NEB	Baseline (M_{mc})	73.1	69.9	25.7	39.0	25.2
	Best (M_{agg+cl})	73.7	71.2	32.1	46.5	31.5
Overall	Baseline (M_{mc})	73.8	70.7	28.5	41.1	28.1
	Best (M_{agg+cl})	74.5	72.0	35.0	48.6	34.5

Table 8: Macro F1 scores for the baseline and best models under the v2 benchmark

point improvement over the baseline’s 27.3%. This increase in overall F1 is primarily driven by the improvement in Location F1, which similarly rises from 27.7% to 33.6%. **These results validate the motivation and impact of our synthetic data.** The best model outperforms the baseline in both EB and NEB scenarios. However, as discussed in Section 4.4 regarding the importance of performance on EB, there remains room for improvement: the best model reaches only 61.6%, in spite of the increase from the baseline’s 53.2%. **This insight can inform further error analysis and targeted improvements in future models for this task.**

Turning to the macro scores in Table 8, we observe an increase across all metrics compared to the micro scores, but the same trends persist. The best model achieves an overall F1 of 34.5% on the overall test set, a notable 6.4 percentage-point improvement over the baseline’s 28.1%. For Shape F1 on the overall test set, the best model scores 42.2% (micro) and 48.6% (macro), up from the baseline’s 36.3% and 41.1%, marking significant gains of 5.9 and 7.5 percentage points, respectively.

7.2 Qualitative evaluation

We present examples of output from both the baseline and best models, demonstrating the substantial improvement of the latter. For each example, we also discuss the overall F1 metric and relevant auxiliary metrics. A complete table of scores for all metrics across examples is provided in the appendix (Table 10).

Example 1. As shown in Figure 17, copying substructures is a common strategy in the MDC. Here, **A** instructs **B** to build an arrowhead, asking **B** to "mirror" the completed half on the opposite side. The baseline model only captures the "on the top" aspect of this

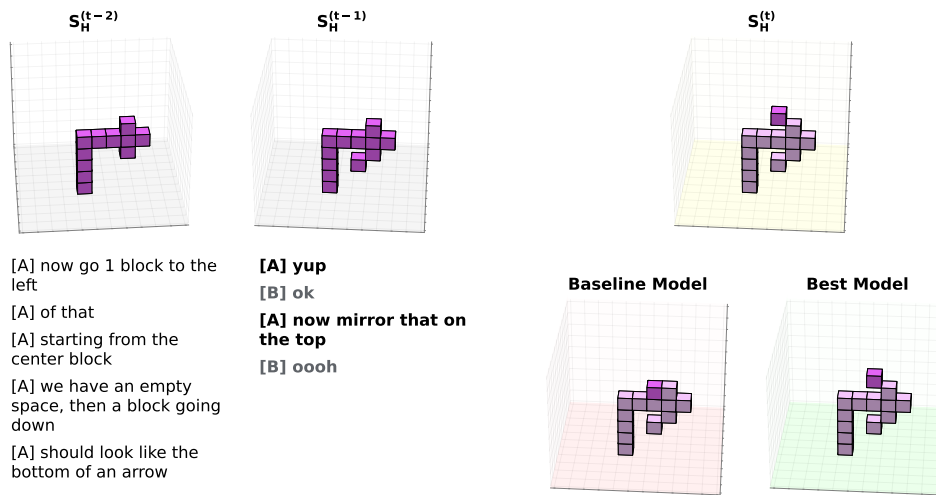


Figure 17: Example 1

instruction, while the best model fully understands and completes the arrowhead. This example also involves placing a floating block. The best model accomplishes this too, by placing and then removing a supporting block (not shown in the figure). It achieves an overall F1 score of 1.0, compared to the baseline model's 0. However, both models achieve perfect type and color F1 scores, as the baseline model correctly identifies the need for a single purple block to be placed (in terms of net actions).

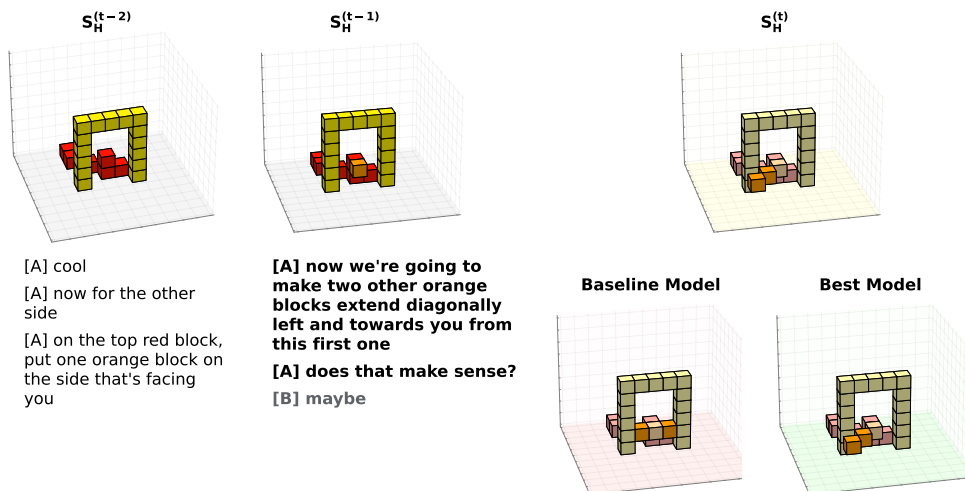


Figure 18: Example 2

Example 2. As shown in Figure 18, A gives a complex instruction requiring blocks to meet several highly specific criteria, including a criterion involving the builder's position

and orientation. The baseline model only grasps the "two other orange blocks" aspect but poorly interprets their placement. In contrast, the best model fully understands the instruction. Similar to the previous example, this example also involves placing floating blocks, which the best model accomplishes successfully. It achieves an overall F1 score of 1.0, compared to the baseline model's 0. However, both models achieve perfect type and color F1 scores, as the baseline model correctly identifies the need for two orange blocks to be placed (in terms of net actions).

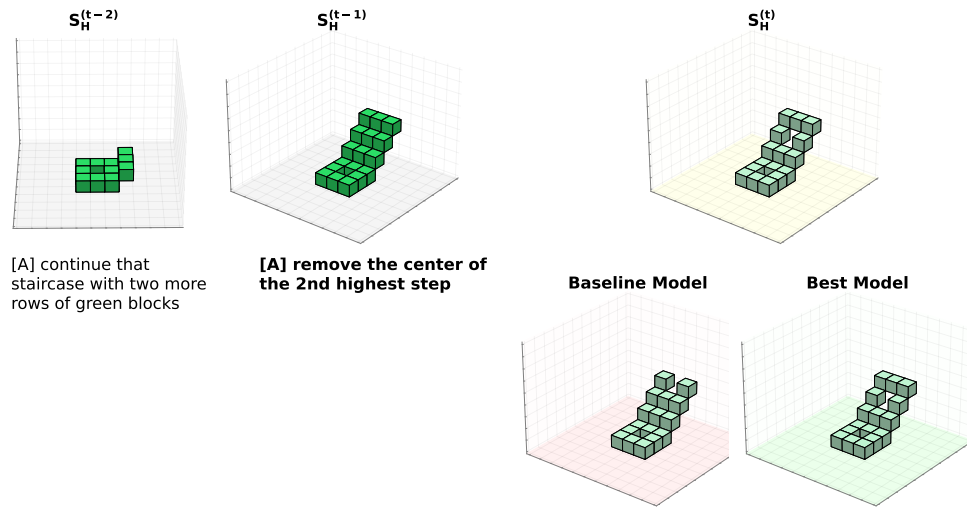


Figure 19: Example 3

Example 3. As shown in Figure 19, this example mirrors the previous one but focuses on block removals instead of placements. The initial structure, S_H^{t-1} , consists of three steps extending from a base square. **A** instructs **B** to remove a very specific block, using terms like "center" and "second highest step" to describe its location. The baseline model incorrectly selects the third highest step instead of the second, while the best model interprets the instruction accurately. The latter achieves an overall F1 score of 1.0, compared to the former's 0. However, both models achieve perfect type and color F1 scores, as the baseline model correctly identifies the need to remove one green block.

8. Discussion

We now discuss four topics in detail: an additional key challenge in BAP evaluation and its implications for future work (Section 8.1), the importance of evaluation on the synthetic data (Section 8.2), relevant concurrent work (Section 8.3), and broader implications of our work that go beyond BAP (Section 8.4).

8.1 An additional key challenge for BAP evaluation

Through manual inspection of random samples during the qualitative analysis of model outputs (Section 7.2), we identified an additional challenge for fair evaluation in the BAP task, separate from the issue addressed by the fairer F1 metric in Section 4.1. Specifically, and rather unsurprisingly, **the F1 metric lacks the sensitivity to distin-**

guish nuanced differences in error quality. It is possible for two models to make different types of errors, with one type being qualitatively "better" than the other – yet the F1 metric may not capture this distinction effectively. This limitation can hinder fair evaluation and reduce our ability to distinguish between models based on their F1 scores. Below, we illustrate this challenge through qualitative examples. Across all examples, the best model M_{agg+cl} consistently performs qualitatively better than the baseline M_{mc} and is arguably closer to the human reference. However, the F1 metric lacks the sensitivity to reflect this substantial quality gap. In some cases, the auxiliary metrics proposed in Section 4.2 offer some help. A full table of scores for all metrics across examples is provided in the appendix (Table 11). It's worth noting that such examples were frequent enough in our random inspection and the ones discussed here are fairly representative of the problem, not cherry-picked to favor the best model.

This analysis underscores the inherent challenges in automated evaluation for the BAP task, highlighting the need for further research in this area. The examples also illustrate the difficulty of creating a clear, unambiguous rubric for grading model output on an absolute scale, making human evaluation equally complex. (In fact, we initially considered human evaluation but ultimately dismissed it due to these challenges.)

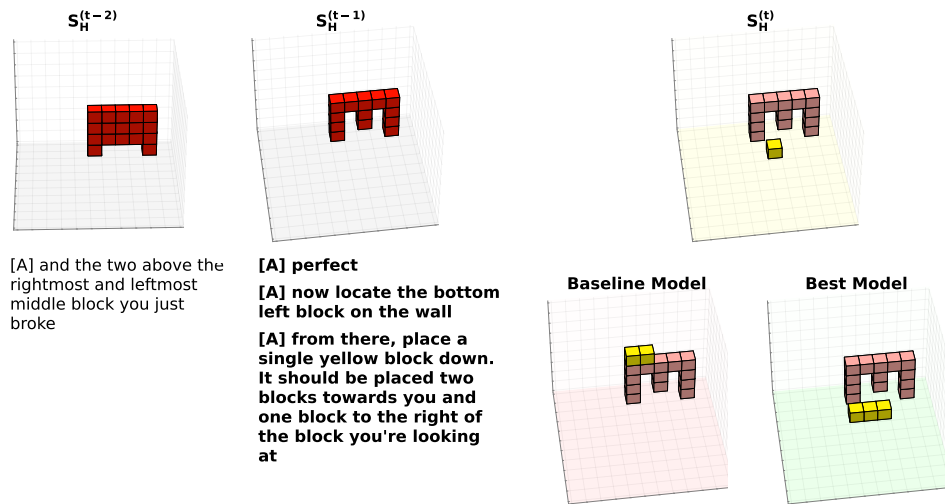


Figure 20: Example A

Example A. As shown in Figure 20, A instructs B to place a yellow block meeting multiple highly specific criteria, including one involving the builder's position and orientation. The best model largely understands these criteria and places the correct block, though it also adds an extraneous one on each side. In contrast, the baseline model performs poorly, producing seemingly random placements.

The F1 metric rates the baseline model as 0 and the best model as 0.5, indicating an improvement. However, this score does not fully capture the qualitative gap between the two models, especially in spatial reasoning. While both models produce two false positives, the errors made by the best model demonstrate a clearer understanding of the task, an aspect that the F1 metric fails to reflect adequately.

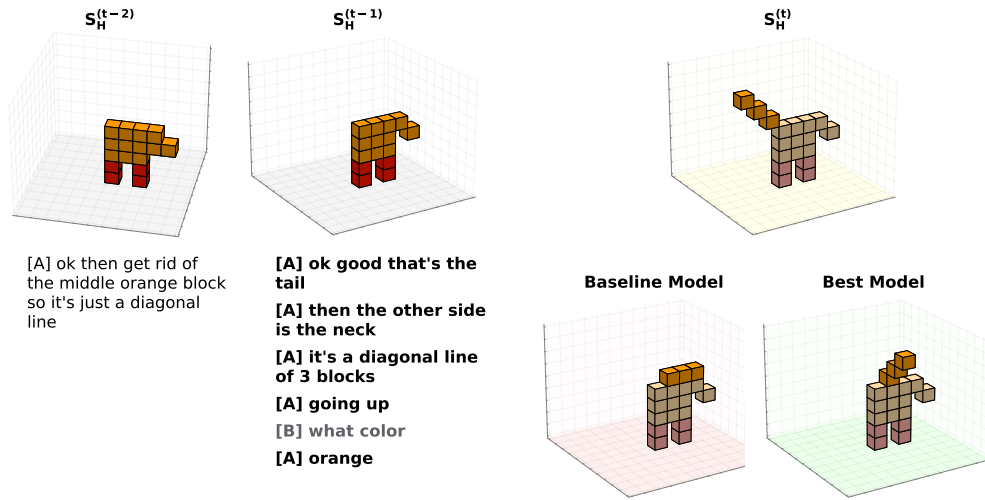


Figure 21: Example B

Example B. As shown in Figure 21, **A** and **B** are building a 2D giraffe, and **A** instructs **B** to place three orange blocks diagonally to form the neck, opposite the tail. The baseline model places three orange blocks, but arranges them horizontally and closer to the tail. While the best model recognizes the need for a diagonal structure, it places it in the wrong location and orientation.

Both models receive an F1 score of 0, with identical scores of 1, 1, and 0 for type, color, and location F1, respectively. However, shape F1 distinguishes the models more effectively: the baseline achieves a shape F1 of 0.33, while the best model achieves a perfect 1.

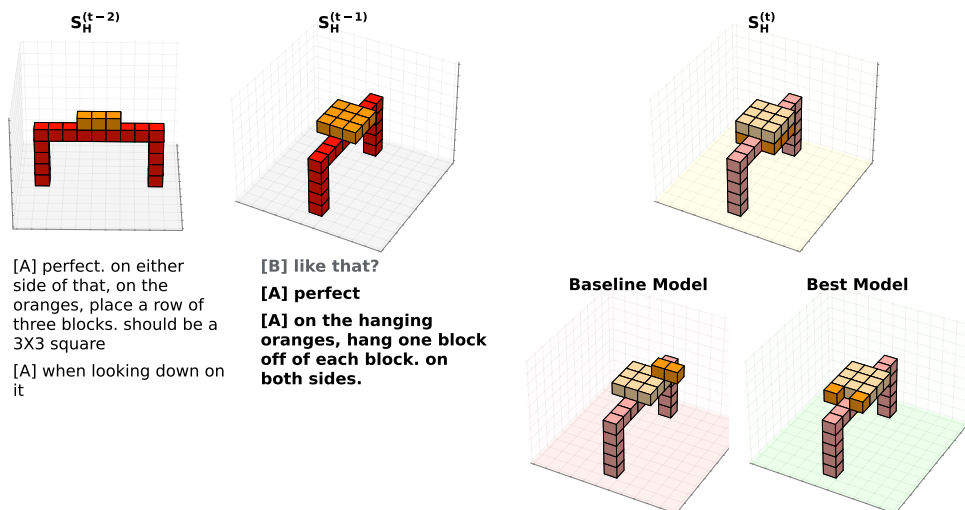


Figure 22: Example C

Example C. As shown in Figure 22, **A** instructs the addition of two rows of orange blocks directly below each hanging row on either side of the arch. The baseline model places two orange blocks on top, while the best model attaches blocks to each hanging row—still incorrect but a noticeably closer interpretation of **A**’s intent.

Here, too, the F1 metric scores both models as 0. Unlike the previous example, however, none of the auxiliary metrics distinguish between the models, as both receive identical scores.

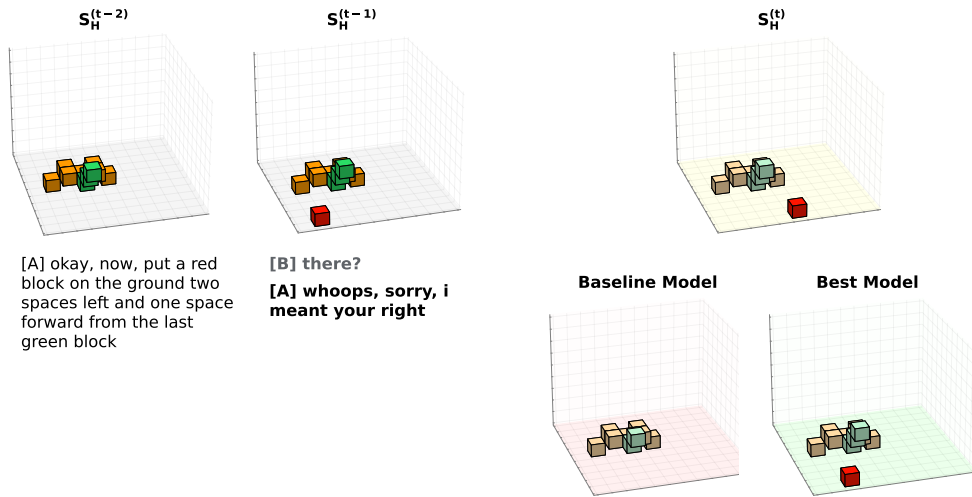


Figure 23: Example D

Example D. As shown in Figure 23, **A** initially directs **B** to place a red block on the left, but then corrects this to the analogous position on the right, requiring removal of the original block and placement of a new one. The baseline model correctly removes the original red block but fails to place a new one, instead removing the top green block randomly. The best model performs only the correct removal and places a new red block to the right, though not in the exact position specified—nonetheless, it is clearly a closer interpretation of **A**’s intent.

In this case, the F1 metric assigns both models a non-zero score of 0.5, as both have 1 true positive, 1 false positive, and 1 false negative. However, the type and color F1 metrics penalize the baseline model, scoring it 0.5 in each, while the best model achieves a perfect score of 1.

8.2 Evaluation on synthetic data

Going forward, evaluation on the synthetic data will also be important for making more meaningful progress on the BAP task. First, the more structured and simpler nature of the synthetic data allows us to assess basic model competencies. Second, as noted in Section 6.1.2, the baseline M_{mc} underperforms significantly on the synthetic datasets, despite being trained on the far more complex D_{mc} data; it even performs worse on datasets D_{ss} and D_r than on D_{mc} . Evaluating on the synthetic data will help build models that do not show such counterintuitive behavior (Section 8.3 provides further evidence supporting this argument), and complements evaluation on D_{mc} . In

fact, future models should aim to surpass previous performance on D_{mc} while also achieving strong results on synthetic data, ideally improving on both.

8.3 Concurrent work

Concurrent to our work are the recently published (at EMNLP, Nov 12-16, 2024) works of [Chaturvedi, Thompson, and Asher \(2024\)](#) and [Kranti, Hakimov, and Schlangen \(2024\)](#), both exploring SOTA LLMs for the BAP task. The former finetunes the Llama-3-8B model ([Dubey et al. 2024](#)) on the original BAP data, resulting in the Nebula model, which predicts the next action sequence in a text-to-text fashion using all preceding conversation and action sequences as context. The latter employs in-context learning with GPT-4. Nebula achieves an F1 score of 39.2% and GPT-4 scores 39.0% (under the now legacy BAP evaluation). Nebula is marginally better, although both are very close and mark improved performance on the task.

As mentioned in Section 1, modeling is not the primary focus of our work. Instead, we focus on the BAP task as a whole, addressing key challenges in data and evaluation to propose BAP v2, an upgraded version of the task itself. We also illustrate the impact of this data on training a simple LLM and transformer-based model. This foundation enables future work to make more efficient and meaningful progress on the task, and sets the stage for more sophisticated models/LLMs. These works are therefore complementary to ours. A slightly more detailed comparison to [Chaturvedi, Thompson, and Asher \(2024\)](#) is provided in the appendix, given some other relevant aspects of their work. We, still, however, evaluate Nebula using our new BAP v2 benchmark to further demonstrate the impact and robustness of our evaluation, and to provide a fairer assessment of its performance. We also evaluate it on our synthetic data to further strengthen our argument about the importance of such evaluation as discussed in Section 8.2. Future work can explore finetuning models such as Llama-3-8B (Nebula) and other SOTA LLMs using our synthetic data and training methodologies like CL.

BAP v2 evaluation. Similar to the 29.4% improvement we observed for our baseline model M_{mc} under the v2 evaluation on D_{mc} , Nebula’s performance also increases from 39.2% to 50.1%, reflecting a 27.8% gain. This further underscores **the impact and robustness of our v2 evaluation**, offering a fairer reflection of Nebula’s performance. Detailed tables for the full v2 benchmark are provided in the appendix (Tables 12 and 13).

Evaluation on the synthetic data. Table 9 shows Nebula’s performance on both the synthetic data (D_{bs} , D_{ss} , D_r) and the original D_{mc} test sets. Evaluating Nebula on the synthetic data reveals behavior consistent with our baseline model M_{mc} , as reported in Section 6.1.2 and further discussed in Section 8.2. It underperforms significantly on the synthetic datasets, despite being trained on the far more complex D_{mc} data; it even performs worse on datasets D_{ss} and D_r than on D_{mc} . This shows that **models trained solely on D_{mc} may not be as robust, and reinforces our argument from Section 8.2 about the importance of synthetic data evaluation**: it will help build models that don’t show such counter-intuitive behavior.

8.4 Broader implications of our work

While our focus in this work is on the Builder Action Prediction (BAP) subtask within the Minecraft Collaborative Building Task (MCBT) setting, the contributions have broader applications and takeaways as well. Below, we discuss their relevance for other

Model	Test Data			
	D_{bs}	D_{ss}	D_r	D_{mc}
Nebula	51.5	33.1	30.9	50.1

Table 9: Nebula’s performance across datasets (and using the v2 evaluation on D_{mc})

subtasks within MCBT, for research building directly on the MCBT, and for similar domains and tasks in the field. This highlights the potential impact of our work and directions for future research.

Within MCBT. Although our primary focus is on BAP, the synthetic data and training methodologies introduced here are applicable to other MCBT subtasks constrained by the limited size of the MDC, such as the Architect Utterance Generation (AUG) subtask (Narayan-Chen, Jayannavar, and Hockenmaier 2019) summarized briefly in Section 2.1.2. AUG and BAP represent two key pillars for building fully interactive Architect and Builder agents. Additionally, other subtasks, such as deciding when the Builder should act versus speak or generating clarification questions during dialogue, could also benefit from our synthetic datasets. Our simulators and data were carefully designed to emulate the nuances of the MCBT itself (Section 5.1), making them directly usable or adaptable to these subtasks. The simulators’ parameterized nature enables generating tailored data distributions to this end, supporting further advancements across the broader MCBT ecosystem.

Beyond MCBT and Related Works. Potential applications of our work also go beyond the MCBT. Several works directly build upon or are inspired by the MCBT/MDC, including IGLU (Mohanty et al. 2024), Bonn et al. (2020), Thompson, Hunter, and Asher (2024), and Bonial et al. (2021). Therefore, future work on them can also potentially benefit from the synthetic data.

For Other Similar Domains and Tasks. Our findings also offer broader takeaways for research on tasks involving grounded, multimodal task-oriented dialogue systems operating in dynamic, spatially complex environments. First, in many realistic scenarios, data collection for complex situated dialogue tasks is often impractical or expensive. Our work illustrates that synthetic data generation can be a viable and scalable alternative to simply collecting more data. Second, we demonstrate that rich synthetic data can be generated for such tasks in game-based or simulated environments like Minecraft by carefully emulating task and game-specific nuances. This approach produces full embodied task oriented dialogues combining utterances, environment actions, and other game state information, offering a viable strategy for similar game-based/simulated and grounded dialog tasks — an underexplored area as highlighted in Section 9.2. Finally, techniques like curriculum learning demonstrate potential and can be explored further in similar domains/tasks in combination with synthetic data.

9. Related Work

9.1 Task and Dataset

The MDC and BAP (Narayan-Chen, Jayannavar, and Hockenmaier 2019; Jayannavar, Narayan-Chen, and Hockenmaier 2020) continue to remain a challenging and relevant testbed for grounded language instruction following. We discuss a few more recent works to highlight this.

Vision-and-Language Navigation (VLN) (Anderson et al. 2018), and its dialog counterpart, Cooperative Vision-and-Dialog Navigation (CVDN) (Thomason et al. 2019), explore instruction following in photorealistic navigation settings. However, Minecraft dialogues are more complex due to their asynchronous communication, longer turn sequences, and dynamic environment changes during construction. Unlike navigation, where referring expressions target existing objects, construction often involves instructions for objects yet to be built. And although more recent navigation tasks require real vision, their underlying world state space (as defined by fixed viewpoints and the underlying navigation graph) is just as highly discretized. Our task does not require vision, but poses an arguably more challenging planning problem, since its action space is much larger (7623 possible actions vs. six actions in the vision-language navigation work). Tasks involving vision and language-based task completion beyond navigation have also been explored. ALFRED (Shridhar et al. 2020) is a benchmark for mapping natural language instructions and egocentric vision to action sequences for household tasks in simulated environments. However, similar to VLN and unlike the MDC, it lacks dialogue and relies solely on planner-based demonstrations instead of human ones. Efforts to combine vision and dialogue navigation with task completion include CEREALBAR (Suhr et al. 2019), which operates in a game-based setting. Yet, similar to CVDN, it uses turn-based dialogue, contrasting with the free-form, asynchronous communication of the MDC.

This limitation is addressed by the more recent benchmark TEACH (Padmakumar et al. 2022), which includes free-form dialogue, similar to the MDC, and features over 3000 human-human interactive dialogues for completing household tasks in simulation and with object state changes. However, unlike the MDC, the instruction giver in TEACH is provided with a predefined plan of steps, while the Architect in the MDC independently devises a unique plan for constructing the target structure. This results in greater creativity and diversity in the MDC, with multiple possible plans for the same structure. Although the TEACH dataset is larger (#dialogs), its dialogues and utterances are shorter. Additionally, the MDC allows for greater abstraction in instructions, such as referring to substructures, individual blocks, or shapes, whereas TEACH focuses on well-defined objects in the environment. Similar to VLN and CVDN, referring expressions in TEACH refer to objects that exist in the world, but construction instructions like those in the MDC frequently refer to objects that need to be built.

Minecraft, in recent years, has garnered a lot of interest as an AI experimentation platform. Our previous work (Narayan-Chen, Jayannavar, and Hockenmaier 2019) was among the first to use it to study grounded task-oriented dialogue, and introduced the MCBT and MDC. Facebook’s CraftAssist (Gray et al. 2019; Jernite et al. 2019; Szlam et al. 2019) is another such example, enabling two-way human-bot interactions where a human architect instructs an automated builder to build complex structures. Their data includes synthetically generated and crowdsourced instructions paired with logical tree structures consisting of action primitives, unlike the MDC, which features human-human dialogues with greater ambiguity, variety, and noisier Builder actions. MineDojo

(Fan et al. 2022) focuses on creating versatile agents for diverse tasks via an internet-scale knowledge base, contrasting with tasks like IGLU (Mohanty et al. 2024; Kiseleva et al. 2022b,a) and MCBT, which prioritize grounded natural language dialogue and clarification for interactive agents.

Among Minecraft-related efforts, IGLU is most closely related to the MDC/MCBT and was directly inspired by it. The IGLU dataset, unlike the MDC, is single turn only, and not dialogue based. It comprises 8136 instruction-action pairs, including 1056 ambiguous instructions with corresponding clarification questions. The task setting is similar to the MCBT but incorporates some simplifications which make it relatively less challenging. E.g., cardinal directions (e.g., North, South) are displayed in the voxel world, which simplifies instruction giving/following through the use of absolute rather than relative references (e.g., left, right). IGLU also introduces a very small multi-turn dataset (127 dialogues) based on this same task setting. It features strict turn-taking and clearly demarcated instructions and clarification questions. This contrasts with the MDC’s free-form, asynchronous dialogues, which are less structured and whose utterances have more diversity.

Some other works also build on or are inspired by the MCBT/MDC. For instance, Bonn et al. (2020), Thompson, Hunter, and Asher (2024), and Bonial et al. (2021) provide additional linguistic annotations for the MDC.

9.2 Synthetic Training Data

Synthetic data has proven beneficial for various tasks, including those mentioned in Section 9.1. VLN agents, constrained by limited human instruction data and diversity in training environments, often struggle with complex language grounding and spatial language understanding. Kamath et al. (2023) address this by using synthetic data, achieving SOTA performance on the RxR dataset (Ku et al. 2020), while Wang et al. (2023) are similar in spirit and achieve SOTA on the aforementioned CVDN and other benchmarks. Similarly, Kang et al. (2023) demonstrate strong performance gains in low-data regimes for Visual Dialog (Das et al. 2017) by leveraging synthetic data. Synthetic data has also been effective for dialogue systems, particularly those focused on text-only dialogues (Kim et al. 2022; Bao et al. 2023; Zhan et al. 2023). Zhan et al. (2024) is an example of extending this to multi-modal dialogue agents, demonstrating the effectiveness of synthetic visual descriptions in enhancing agents’ grounding capabilities.

However, fewer efforts have addressed synthesizing task-oriented embodied dialogues (involving both utterances and environment actions). Padmakumar et al. (2023) were the first to design a framework to do so. They extend agenda-based dialogue simulation (Schatzmann and Young 2009) to a multimodal embodied agent framework, and demonstrate the impact of the synthetic dialogues on the TEACH task (see Section 9.1 for a comparison of TEACH to MDC). Our work serves to provide another useful example in this general domain, further advancing synthetic data generation for such complex tasks. Dan, Han, and Roth (2021) is another closely related work that demonstrates the potential of synthetic data in the Blocks World domain. They use simpler synthetic data for the benchmarks of Bisk, Yuret, and Marcu (2016), which require understanding single-shot instructions that transform one world state to another using simulated 3D blocks. Blocks are viewed from a fixed bird’s eye perspective, initialized randomly in the initial world state, and uniquely identifiable. The varying Builder perspective and lack of easily identifiable referents, along with the need to understand utterances

in a dialogue context, make the BAP task a much more challenging problem.⁷ Our work on synthetic data thus serves as a stronger demonstration of its potential for richer, embodied task-oriented dialogue tasks that extend beyond simpler Blocks World settings.

10. Conclusion and Future Work

In this work, we revisited the challenging Builder Action Prediction (BAP) subtask within the Minecraft Collaborative Building Task (MCBT) setting, addressing key shortcomings in evaluation and training data. We introduced **BAP v2**, an upgraded version of the task, comprising two core contributions: (1) an **enhanced evaluation benchmark** that includes a cleaner test set and fairer, more insightful metrics, and (2) **diverse synthetic training datasets** generated from **novel Minecraft dialogue and target structure simulators**. These contributions together provide a robust foundation for future research on the BAP task. Additionally, our synthetic data demonstrates the potential to train more performant and robust models, even with relatively simple training methods and architectures. Although modeling was not the primary focus of this work, we also illustrated the impact of the synthetic data and training methodologies on training a simple LLM and transformer-based model, thus validating the robustness of our approach, and setting the stage for more sophisticated models/LLMs going forward.

Future work can therefore build on our work to explore more advanced LLMs and architectures while leveraging the BAP v2 framework, alongside training methodologies such as Curriculum Learning (CL). Further improvements could stem from experimenting with more sophisticated CL approaches or entirely new training paradigms to get even more out of the synthetic data. Additionally, as highlighted in Section 8.1, BAP evaluation remains a nuanced challenge, warranting deeper investigation. Finally, Section 8.4 outlined the broader implications of our work, while also highlighting potential directions for future research.

11. Appendix: BAP v2 metrics for Sections 7.2 and 8.1

Example ID	Model	Type	Color	Location	Shape	Overall
Example 1	Baseline	1.0	1.0	0.0	0.0	0.0
	Best	1.0	1.0	1.0	1.0	1.0
Example 2	Baseline	1.0	1.0	0.0	0.5	0.0
	Best	1.0	1.0	1.0	1.0	1.0
Example 3	Baseline	1.0	1.0	0.0	0.0	0.0
	Best	1.0	1.0	1.0	1.0	1.0

Table 10: BAP v2 metrics by Example ID for Section 7.2 (range [0, 1])

⁷ Also, unlike traditional Blocks World, Minecraft allows blocks to float (requiring non-monotonic action sequences where placement is followed by removal), or attach to any side of an existing block.

Example ID	Model	Type	Color	Location	Shape	Overall
Example A	Baseline	0.67	0.67	0.0	0.0	0.0
	Best	0.5	0.5	0.5	0.5	0.5
Example B	Baseline	1.0	1.0	0.0	0.33	0.0
	Best	1.0	1.0	0.0	1.0	0.0
Example C	Baseline	0.5	0.5	0.0	0.0	0.0
	Best	0.5	0.5	0.0	0.0	0.0
Example D	Baseline	0.5	0.5	0.5	0.0	0.5
	Best	1.0	1.0	0.5	0.0	0.5

Table 11: BAP v2 metrics by Example ID for Section 8.1 (range [0, 1])

12. Appendix: Concurrent work

Dataset	Type	Color	Location	Shape	Overall
EB	92.8	92.8	78.3	84.8	78.3
NEB	79.0	77.4	47.2	59.0	46.4
Overall	80.6	79.1	50.7	61.9	50.1

Table 12: Micro F1 scores for the Nebula model under the v2 benchmark

Dataset	Type	Color	Location	Shape	Overall
EB	96.8	96.8	84.5	90.5	84.5
NEB	81.7	80.9	47.1	64.1	46.5
Overall	82.9	82.2	50.1	66.3	49.6

Table 13: Macro F1 scores for the Nebula model under the v2 benchmark

References

- Anderson, Peter, Qi Wu, Damien Teney, Jake Bruce, Mark Johnson, Niko Sünderhauf, Ian D. Reid, Stephen Gould, and Anton van den Hengel. 2018. Vision-and-language navigation: Interpreting visually-grounded navigation instructions in real environments. In *2018 IEEE Conference on Computer Vision and Pattern Recognition, CVPR 2018, Salt Lake City, UT, USA, June 18-22, 2018*, pages 3674–3683, IEEE Computer Society.
- Bao, Jianzhu, Rui Wang, Yasheng Wang, Aixin Sun, Yitong Li, Fei Mi, and Ruifeng Xu. 2023. A synthetic data generation framework for grounded dialogues. In *Proceedings of the 61st Annual Meeting of the Association for Computational Linguistics (Volume 1: Long Papers)*, pages 10866–10882, Association for Computational Linguistics, Toronto, Canada.
- Bengio, Yoshua, Jérôme Louradour, Ronan Collobert, and Jason Weston. 2009. Curriculum learning. In *Proceedings of the 26th Annual International Conference on Machine Learning, ICML '09*, page 41–48, Association for Computing Machinery, New York, NY, USA.
- Bisk, Yonatan, Deniz Yuret, and Daniel Marcu. 2016. Natural language communication with robots. In *Proceedings*

- of the 2016 Conference of the North American Chapter of the Association for Computational Linguistics: Human Language Technologies, pages 751–761, Association for Computational Linguistics, San Diego, California.
- Bonial, Claire, Mitchell Abrams, David Traum, and Clare Voss. 2021. Builder, we have done it: Evaluating & extending dialogue-AMR NLU pipeline for two collaborative domains. In *Proceedings of the 14th International Conference on Computational Semantics (IWCS)*, pages 173–183, Association for Computational Linguistics, Groningen, The Netherlands (online).
- Bonn, Julia, Martha Palmer, Zheng Cai, and Kristin Wright-Bettner. 2020. Spatial AMR: Expanded spatial annotation in the context of a grounded Minecraft corpus. In *Proceedings of the Twelfth Language Resources and Evaluation Conference*, pages 4883–4892, European Language Resources Association, Marseille, France.
- Chaturvedi, Akshay, Kate Thompson, and Nicholas Asher. 2024. Nebula: A discourse aware Minecraft builder. In *Findings of the Association for Computational Linguistics: EMNLP 2024*, pages 6431–6443, Association for Computational Linguistics, Miami, Florida, USA.
- Cho, Kyunghyun, Bart van Merriënboer, Caglar Gulcehre, Dzmitry Bahdanau, Fethi Bougares, Holger Schwenk, and Yoshua Bengio. 2014. Learning phrase representations using RNN encoder–decoder for statistical machine translation. In *Proceedings of the 2014 Conference on Empirical Methods in Natural Language Processing (EMNLP)*, pages 1724–1734, Association for Computational Linguistics, Doha, Qatar.
- Dan, Soham, Xinran Han, and Dan Roth. 2021. Compositional data and task augmentation for instruction following. In *Findings of the Association for Computational Linguistics: EMNLP 2021*, pages 2076–2081, Association for Computational Linguistics, Punta Cana, Dominican Republic.
- Das, Abhishek, Satwik Kottur, Khushi Gupta, Avi Singh, Deshraj Yadav, José M.F. Moura, Devi Parikh, and Dhruv Batra. 2017. Visual Dialog. In *Proceedings of the IEEE Conference on Computer Vision and Pattern Recognition (CVPR)*, pages 326–335.
- Devlin, Jacob, Ming-Wei Chang, Kenton Lee, and Kristina Toutanova. 2019. BERT: Pre-training of deep bidirectional transformers for language understanding. In *Proceedings of the 2019 Conference of the North American Chapter of the Association for Computational Linguistics: Human Language Technologies, Volume 1 (Long and Short Papers)*, pages 4171–4186, Association for Computational Linguistics, Minneapolis, Minnesota.
- Dubey, Abhimanyu, Abhinav Jauhri, Abhinav Pandey, Abhishek Kadian, Ahmad Al-Dahle, Aiesha Letman, Akhil Mathur, Alan Schelten, Amy Yang, Angela Fan, et al. 2024. The llama 3 herd of models. *arXiv preprint arXiv:2407.21783*.
- Fan, Linxi, Guanzhi Wang, Yunfan Jiang, Ajay Mandlekar, Yuncong Yang, Haoyi Zhu, Andrew Tang, De-An Huang, Yuke Zhu, and Anima Anandkumar. 2022. Minedojo: Building open-ended embodied agents with internet-scale knowledge. In *Advances in Neural Information Processing Systems*, volume 35, pages 18343–18362, Curran Associates, Inc.
- Gray, Jonathan, Kavya Srinet, Yacine Jernite, Haonan Yu, Zhuoyuan Chen, Demi Guo, Siddharth Goyal, C. Lawrence Zitnick, and Arthur Szlam. 2019. CraftAssist: A framework for dialogue-enabled interactive agents. *arXiv preprint arXiv:1907.08584*.
- Jayannavar, Prashant, Anjali Narayan-Chen, and Julia Hockenmaier. 2020. Learning to execute instructions in a Minecraft dialogue. In *Proceedings of the 58th Annual Meeting of the Association for Computational Linguistics*, pages 2589–2602, Association for Computational Linguistics, Online.
- Jernite, Yacine, Kavya Srinet, Jonathan Gray, and Arthur Szlam. 2019. CraftAssist instruction parsing: Semantic parsing for a Minecraft assistant. *arXiv preprint arXiv:1905.01978*.
- Johnson, Matthew, Katja Hofmann, Tim Hutton, and David Bignell. 2016. The Malmö platform for artificial intelligence experimentation. In *Proceedings of the Twenty-Fifth International Joint Conference on Artificial Intelligence (IJCAI-16)*, pages 4246–4247.
- Kamath, Aishwarya, Peter Anderson, Su Wang, Jing Yu Koh, Alexander Ku, Austin Waters, Yinfei Yang, Jason Baldridge, and Zarana Parekh. 2023. A new path: Scaling vision-and-language navigation with synthetic instructions and imitation learning. In *Proceedings of the IEEE/CVF Conference on Computer Vision and Pattern Recognition (CVPR)*, pages 10813–10823.

- Kang, Gi-Cheon, Sungdong Kim, Jin-Hwa Kim, Donghyun Kwak, and Byoung-Tak Zhang. 2023. The dialog must go on: Improving visual dialog via generative self-training. In *Proceedings of the IEEE/CVF Conference on Computer Vision and Pattern Recognition (CVPR)*, pages 6746–6756.
- Kim, Gangwoo, Sungdong Kim, Kang Min Yoo, and Jaewoo Kang. 2022. Generating information-seeking conversations from unlabeled documents. In *Proceedings of the 2022 Conference on Empirical Methods in Natural Language Processing*, pages 2362–2378, Association for Computational Linguistics, Abu Dhabi, United Arab Emirates.
- Kiseleva, Julia, Ziming Li, Mohammad Aliannejadi, Shrestha Mohanty, Maartje ter Hoeve, Mikhail Burtsev, Alexey Skrynnik, Artem Zhulus, Aleksandr Panov, Kavya Srinet, Arthur Szlam, Yuxuan Sun, Katja Hofmann, Marc-Alexandre Côté, Ahmed Awadallah, Linar Abdrazakov, Igor Churin, Putra Manggala, Kata Naszadi, Michiel van der Meer, and Taewoon Kim. 2022a. Interactive grounded language understanding in a collaborative environment: Iglu 2021. In *Proceedings of the NeurIPS 2021 Competitions and Demonstrations Track*, volume 176 of *Proceedings of Machine Learning Research*, pages 146–161, PMLR.
- Kiseleva, Julia, Alexey Skrynnik, Artem Zhulus, Shrestha Mohanty, Negar Arabzadeh, Marc-Alexandre Côté, Mohammad Aliannejadi, Milagro Teruel, Ziming Li, Mikhail Burtsev, Maartje ter Hoeve, Zoya Volovikova, Aleksandr Panov, Yuxuan Sun, Kavya Srinet, Arthur Szlam, Ahmed Awadallah, Seungeun Rho, Taehwan Kwon, Daniel Wontae Nam, Felipe Bivort Haiek, Edwin Zhang, Linar Abdrazakov, Guo Qingyam, Jason Zhang, and Zhibin Guo. 2022b. Interactive grounded language understanding in a collaborative environment: Retrospective on iglu 2022 competition. In *Proceedings of the NeurIPS 2022 Competitions Track*, volume 220 of *Proceedings of Machine Learning Research*, pages 204–216, PMLR.
- Köhn, Arne, Julia Wichlacz, Christine Schäfer, Álvaro Torralba, Joerg Hoffmann, and Alexander Koller. 2020. MC-saar-instruct: a platform for Minecraft instruction giving agents. In *Proceedings of the 21th Annual Meeting of the Special Interest Group on Discourse and Dialogue*, pages 53–56, Association for Computational Linguistics, 1st virtual meeting.
- Kranti, Chalamalasetti, Sherzod Hakimov, and David Schlangen. 2024. Retrieval-augmented code generation for situated action generation: A case study on Minecraft. In *Findings of the Association for Computational Linguistics: EMNLP 2024*, pages 11159–11170, Association for Computational Linguistics, Miami, Florida, USA.
- Ku, Alexander, Peter Anderson, Roma Patel, Eugene Ie, and Jason Baldridge. 2020. Room-across-room: Multilingual vision-and-language navigation with dense spatiotemporal grounding. In *Proceedings of the 2020 Conference on Empirical Methods in Natural Language Processing (EMNLP)*, pages 4392–4412, Association for Computational Linguistics, Online.
- Mohanty, Shrestha, Negar Arabzadeh, Andrea Tupini, Yuxuan Sun, Alexey Skrynnik, Artem Zhulus, Marc-Alexandre Côté, and Julia Kiseleva. 2024. Idat: A multi-modal dataset and toolkit for building and evaluating interactive task-solving agents. *arXiv preprint arXiv:2407.08898*.
- Narayan-Chen, Anjali, Prashant Jayannavar, and Julia Hockenmaier. 2019. Collaborative dialogue in Minecraft. In *Proceedings of the 57th Annual Meeting of the Association for Computational Linguistics*, pages 5405–5415, Association for Computational Linguistics, Florence, Italy.
- Ogawa, Haruna, Hitoshi Nishikawa, Takenobu Tokunaga, and Hikaru Yokono. 2020. Gamification platform for collecting task-oriented dialogue data. In *Proceedings of the Twelfth Language Resources and Evaluation Conference*, pages 7084–7093, European Language Resources Association, Marseille, France.
- Padmakumar, Aishwarya, Mert Inan, Spandana Gella, Patrick Lange, and Dilek Hakkani-Tur. 2023. Multimodal embodied plan prediction augmented with synthetic embodied dialogue. In *Proceedings of the 2023 Conference on Empirical Methods in Natural Language Processing*, pages 6114–6131, Association for Computational Linguistics, Singapore.
- Padmakumar, Aishwarya, Jesse Thomason, Ayush Shrivastava, Patrick Lange, Anjali Narayan-Chen, Spandana Gella, Robinson PIRAMUTHU, Gokhan Tur, and Dilek Hakkani-Tur. 2022. Teach: Task-driven embodied agents that chat. *Proceedings of*

- the AAAI Conference on Artificial Intelligence*, 36(2):2017–2025.
- Pennington, Jeffrey, Richard Socher, and Christopher Manning. 2014. GloVe: Global vectors for word representation. In *Proceedings of the 2014 Conference on Empirical Methods in Natural Language Processing*, pages 1532–1543, Association for Computational Linguistics, Doha, Qatar.
- Schatzmann, Jost and Steve Young. 2009. The hidden agenda user simulation model. *IEEE Transactions on Audio, Speech, and Language Processing*, 17(4):733–747.
- Shridhar, Mohit, Jesse Thomason, Daniel Gordon, Yonatan Bisk, Winson Han, Roozbeh Mottaghi, Luke Zettlemoyer, and Dieter Fox. 2020. Alfred: A benchmark for interpreting grounded instructions for everyday tasks. In *Proceedings of the IEEE/CVF Conference on Computer Vision and Pattern Recognition (CVPR)*.
- Suhr, Alane, Claudia Yan, Jack Schluger, Stanley Yu, Hadi Khader, Marwa Mouallem, Iris Zhang, and Yoav Artzi. 2019. Executing instructions in situated collaborative interactions. In *Proceedings of the 2019 Conference on Empirical Methods in Natural Language Processing and the 9th International Joint Conference on Natural Language Processing (EMNLP-IJCNLP)*, pages 2119–2130, Association for Computational Linguistics, Hong Kong, China.
- Sutskever, Ilya, Oriol Vinyals, and Quoc V Le. 2014. Sequence to sequence learning with neural networks. In *Advances in neural information processing systems*, pages 3104–3112.
- Szlam, Arthur, Jonathan Gray, Kavya Srinet, Yacine Jernite, Armand Joulin, Gabriel Synnaeve, Douwe Kiela, Haonan Yu, Zhuoyuan Chen, Siddharth Goyal, Demi Guo, Danielle Rothermel, C. Lawrence Zitnick, and Jason Weston. 2019. Why build an assistant in Minecraft? *arXiv preprint arXiv:1907.09273*.
- Thomason, Jesse, Michael Murray, Maya Cakmak, and Luke Zettlemoyer. 2019. Vision-and-dialog navigation. *arXiv preprint arXiv:1907.04957*.
- Thompson, Kate, Julie Hunter, and Nicholas Asher. 2024. Discourse structure for the Minecraft corpus. In *Proceedings of the 2024 Joint International Conference on Computational Linguistics, Language Resources and Evaluation (LREC-COLING 2024)*, pages 4957–4967, ELRA and ICCL, Torino, Italia.
- Turc, Iulia, Ming-Wei Chang, Kenton Lee, and Kristina Toutanova. 2019. Well-read students learn better: On the importance of pre-training compact models. *arXiv preprint arXiv:1908.08962v2*.
- Vaswani, Ashish, Noam Shazeer, Niki Parmar, Jakob Uszkoreit, Llion Jones, Aidan N Gomez, Łukasz Kaiser, and Illia Polosukhin. 2017. Attention is all you need. In *Advances in Neural Information Processing Systems*, volume 30, Curran Associates, Inc.
- Wang, Zun, Jialu Li, Yicong Hong, Yi Wang, Qi Wu, Mohit Bansal, Stephen Gould, Hao Tan, and Yu Qiao. 2023. Scaling data generation in vision-and-language navigation. In *Proceedings of the IEEE/CVF International Conference on Computer Vision (ICCV)*, pages 12009–12020.
- Winograd, Terry. 1971. Procedures as a representation for data in a computer program for understanding natural language. Technical report, MIT. Cent. Space Res.
- Xu, Benfeng, Licheng Zhang, Zhendong Mao, Quan Wang, Hongtao Xie, and Yongdong Zhang. 2020. Curriculum learning for natural language understanding. In *Proceedings of the 58th Annual Meeting of the Association for Computational Linguistics*, pages 6095–6104, Association for Computational Linguistics, Online.
- Zhan, Haolan, Sameen Maruf, Lizhen Qu, Yufei Wang, Ingrid Zukerman, and Gholamreza Haffari. 2023. Turning flowchart into dialog: Augmenting flowchart-grounded troubleshooting dialogs via synthetic data generation. In *Proceedings of the 21st Annual Workshop of the Australasian Language Technology Association*, pages 88–99, Association for Computational Linguistics, Melbourne, Australia.
- Zhan, Haolan, Sameen Maruf, Ingrid Zukerman, and Gholamreza Haffari. 2024. Going beyond imagination! enhancing multi-modal dialogue agents with synthetic visual descriptions. In *Proceedings of the 25th Annual Meeting of the Special Interest Group on Discourse and Dialogue*, pages 420–427, Association for Computational Linguistics, Kyoto, Japan.
- Zholus, Artem, Alexey Skrynnik, Shrestha Mohanty, Zoya Volovikova, Julia Kiseleva, Artur Szlam, Marc-Alexandre Coté, and Aleksandr I Panov. 2022. Iglu gridworld: Simple and fast environment for embodied dialog agents. *arXiv preprint*

arXiv:2206.00142.